ISTITUTO NAZIONALE DI FISICA NUCLEARE
Sezione di Genova

INFN-19-10/GE

Particle Astrophysics in Space with an Antimatter Large Acceptance Detector in Orbit (ALADINO)

O. Adriani[1,2], G. Ambrosi[3], P. Azzarello[4], B. Baoudoy[5], L. Basara[6], F. Bindel[7], A. Bonelli[5], M. Boezio[8], V. Bonvicini[8], S. Bottai[2], R. Bruce[5], W.J. Burger[6], A. Contin[9], F. Cadoux[4], V. Calvelli[10], D. Campana[11], R. D'Alessandro[1,2], A. De Benedittis[12,13], L. Derome[14], I. De Mitri[20,21], F. Dimiccoli[6,15], M. Duranti[3,16], S. Farinon[10], E. Fiandrini[3,16], V. Formato[3], F. Gargano[17], I. Gebauer[7], M. Ionica[3], R. Iuppa[6,15], F.P. Juster[5], K. Kanishev[6], I. Lazzizzera[6,15], F. Loparco[17,18], D. Maurin[14], G. Marsella[12,13], N. Masi[9], M.N. Mazziotta[17], R. Musenich[10], M. Paniccia[4], G. Osteria[11], P. Papini[3], M. Pierce[19], L. Quadrani[9], P. Saracco[10], N. Tomassetti[3,16], A. Surdo[13], V. Vagelli[3], M. Weinreuter[7], X. Wu[4], S. Zeissler[7]

1) *Dipartimento di Fisica, Università di Firenze via Sansone 1, 50019 Sesto Fiorentino (Firenze), Italy*
2) *INFN-Sezione di Firenze, via Sansone 1, 50019 Sesto Fiorentino (Firenze),Italy*
3) *INFN- Sezione di Perugia, via A.Pascoli, 06123, Perugia, Italy*
4) *University of Geneva, Quai Ernest-Ansermet 30, 1211 Genève 4, Switzerland*
5) *CEA Saclay Irfu/SACM, Saclay, France*
6) *INFN-TIFPA, Via Sommarive 14, 38123 Povo (Trento), Italy*
7) *KIT, Karlsruher Institut für Technologie, Karlsruhe, Germany*
8) *INFN- Sezione di Trieste, via Valerio 2 - 34127 Trieste Italy*
9) *Università e INFN Bologna, Viale Carlo Berti Pichat, 6/2, 40127 Bologna, Italy*
10) *INFN- Sezione di Genova, via Dodecaneso 33, Genova, Italy*
11) *INFN- Sezione di Napoli, complesso Universitario Monte Sant'Angelo Ed.G, Via Cintia, 80126 Napoli, Italy*
12) *Università del Salento, Via per Arnesano, 73100 Lecce,Italy*
13) *INFN- Sezione di Lecce, Via per Arnesano, 73100 Lecce, Italy*
14) *Universitè Grenoble Alpes and IN2P3 LSPC, 53 Avenue des Martyrs, 38026 Grenoble, France*
15) *Dipartimento di Fisica, Università di Trento, Italy*
16) *Dipartimento di Fisica, Università di Perugia, Italy*
17) *INFN- Sezione di Bari, via Orabona 4, I-70126 Bari, Italy Italy*
18) *Dipartimento di Fisica M. Merlin, Università e Politecnico di Bari, via Amendola 173, I-70126 Bari, Italy*
19) *KTH Royal Institute of Technology, Stockholm, Sweden*
20) *GSSI, Gran Sasso Science Institute - Viale F. Crispi, 7 67100 L'Aquila, Italy*
21) *INFN - Laboratori Nazionali del Gran Sasso, Assergi (L'Aquila), Italy*

Abstract

The note describes a proposal for a large acceptance magnetic spectrometer based on a novel superconducting magnet technology, equipped with a silicon tracker and a 3D isotropic calorimeter.

ALADINO (Antimatter Large Acceptance Detector IN Orbit) is conceived to study anti-matter components of the cosmic radiation in an unexplored energy window which can shed light on new phenomena related to the origin and evolution of the Universe, as well as on the origin and propagation of cosmic rays in our galaxy.

The main science themes addressed by this mission are therefore the origin and composition of the Universe (by means of direct search for primordial anti-nuclei in the Cosmic Ray (CR) flux and indirect search for Dark Matter signals in the CR anti-particle fluxes) as well as the origin and propagation of CR in the Galaxy (by means of precise measurements of the energy spectra and chemical composition of the CR).

1 INTRODUCTION

As of today, anti-deuteron and anti-helium are the heaviest antimatter objects observed so far, and only at accelerators. However, theories that predict either the existence of antimatter in segregated domains or its total absence have no firm foundation in experimental data. The detection of $|Z|>2$ antinuclei in CRs would then shatter our current understanding of cosmology or reveal something unforeseen in the realm of astrophysical objects. The existence of dark matter (DM) is by now well established by a variety of astrophysical and cosmological observations, but its particle nature is still subject of exciting speculations. Indirect searches of DM particles aim at detecting signature of their annihilation/decay as an excess in the CR flux with respect to standard astrophysical expectations. The key point is to look for species and energies where the tiny DM signal can beat the astrophysical background. Antiparticles constitute a golden channel for this search. However, the estimation of the astrophysical background demands a substantial gain of knowledge in CR astrophysics. We propose a large acceptance magnetic space spectrometer aiming at fully characterizing the cosmic radiation up to PeV energies, the so-called “knee” region, where a flux transition from galactic to extragalactic CR sources is expected.

The above-mentioned scientific questions set the key performance parameters for the mission. Access to space is mandatory to avoid atmospheric background and to ensure the desired observation time. A collection factor of ~15 m^2 sr yr, a maximum detectable rigidity of 20 TV, and a $e^{\pm}/p^{\pm}$ separation at the level of 10^6 are mandatory to drive a substantial advance in the field. Velocity measurement with 1% resolution allows of anti-deuteron detection in the energy range where DM signals are expected. No antimatter/matter separation is needed to study the CR spectrum at E~1 PeV, but a collection factor of 20 m^2 sr yr is required to collect enough statistics due to the low CR flux intensity at the highest energies.

All these performance requirements combine in the ALADINO (Antimatter Large Acceptance Detector IN Orbit) concept, designed for a five-year mission in high Earth orbit or L2 orbital position to maximize the CR collection while minimizing active cooling. The apparatus is characterized by a novel isotropic design to maximize the acceptance while keeping under control the overall weight (M~6.6Ton) and size (a cylinder of 4.4 m in diameter and 2m in length). Particles and antiparticles are distinguished by their bending in opposite directions in a magnetic spectrometer. Six layers of silicon detectors track the CR trajectories with a precision of 3 μm over a path length of ≈1.7 m within the ~0.8 T average magnetic field generated by a superconducting toroid. Above and below the tracker, scintillator planes constitute the Time-of-Flight (ToF) detector, which measures the CR arrival directions and velocities, providing fast trigger signals. The tracker layers and the ToF planes ensure multiple charge measurements. The spectrometer surrounds a 3D, 61 radiation lengths deep homogeneous calorimeter that provides energy measurement, $e^{\pm}/p^{\pm}$ discrimination and fast trigger logic configuration. The ALADINO sub-detectors are based on well-known technology developed for high-energy physics

experiments and have a high TRL: silicon sensors, scintillators, and homogeneous calorimeters have been successfully operated in long-term space missions in the past. The major challenge will be the design and operation of the superconducting magnet, the cryogenics and thermal design of the payload. The ALADINO concept is based on a high temperature titanium clad magnesium diboride (MgB_2) superconductor operating at 10-20 K. A prototype of this conductor for space applications was developed under the EU-FP7 project SR2S, but an intense R&D program will be needed to reach the level of readiness for a mission in a 15-20 year timeline. Although this program is highly ambitious, the development of new technologies for high-temperature superconducting magnets is of increasing interest for space applications and for radiation shielding in long-term manned missions.

2 SCIENCE CASE

Cosmic rays (CRs) are a direct sample of solar, galactic, and extragalactic matter that includes all known nuclei and their isotopes, as well as electrons and antiparticles. Their energy spectrum extends several orders of magnitude from ~10^6 eV to about ~10^{21} eV. The origin of CRs, their acceleration mechanisms, and their subsequent propagation toward Earth have intrigued scientists since their discovery. The connections of CRs with fundamental physics topics are of particular interest. Examples are the nature of cosmological dark matter or the unexplained asymmetry between antimatter and matter in our Universe.

The detection of high-energy antiparticles in the cosmic radiation may have strong consequences for cosmology and particle physics. Antimatter is very rare in today's visible Universe: antiparticles produced in the big bang seem to have disappeared in annihilation reactions. At extragalactic scales, large concentrations of antimatter could still exist but no evidence has been found yet [1].

At the Galactic scale, antiparticles may be produced by annihilation or decay of dark matter (DM) particles. The nature of the DM is one of the unsolved problems in modern astrophysics and this has motivated the search for antiparticles in many CR detection experiments. However, a claim of DM signature from these indirect measurements is very challenging, because antiparticles are also created by collisions of ordinary CRs with the gas nuclei in the interstellar medium (ISM). For example, collisions of CR protons with the interstellar hydrogen can produce positrons or antiprotons. The level of antimatter arising from these collisions has to be carefully calculated, as it constitutes the astrophysical background for the DM search [2] [33]. These calculations crucially depend on our knowledge of CR acceleration and propagation processes through the Galaxy, which is as yet poorly understood. It is believed that CRs at least up to about 10^{17} eV are accelerated by Galactic sources, such as supernova remnants, via diffusive shock acceleration mechanisms [3]. In their subsequent transport in the turbulent magnetic fields of the Galaxy, CRs propagate diffusively and remain confined within the Galactic halo for ~1-10 million years. During propagation, the particles undergo energy changes and hadronic

interactions with the gas nuclei of the ISM. These interactions produce new, rare, CR particles such as ^{2}H or ^{3}He isotopes, Li-Be-B nuclei, and antiparticles [4].

Finally, CRs detected at Earth are also affected by the solar wind, which significantly "modulates" the shape of their energy spectrum, below a few tens of GeV, in a time-dependent way. Solar modulation effects are related to the level of solar activity and its magnetic polarity, although the relevance of the various processes of particle transport in the heliosphere is not yet properly understood [5].

The ALADINO project aims at determining key physics properties of the cosmic radiation: energy spectrum, elemental/isotopic composition, arrival directions, and temporal variations.

This investigation addresses highly-demanded science questions at the interface between particle physics and cosmology:

What's the origin of the antimatter-matter asymmetry in our Universe?

What is the particle nature of dark matter? Does it contribute to the cosmic radiation?

What are the sources of CRs? How and where are they accelerated?

How do they propagate through the Galaxy? What kind of interactions do they experience?

To what extent extragalactic particles contribute to the CR flux?

What are the physics processes that rule CR transport in the heliosphere?

The ultimate physics goal of the ALADINO experiment is the systematic investigation and eventual resolution of all above open questions.

The rest of this section is devoted to better illustrate the physical motivations for the ALADINO project.

2.1 Nuclear antimatter

In spite of large efforts in antimatter search in the last decades [6][20][63], antimatter nuclei have not been observed in CRs so far. The detection of heavy anti-nuclei (with mass number $A>3$ or charge $Z<-2$) would have a profound impact on our understanding of the Universe. The lack of clear signatures in gamma-ray sky surveys has led many authors to conclude that the distance to any hypothetical domain of primordial antimatter must be roughly comparable to the horizon scale [7]. The generally accepted theory to explain a baryon asymmetric Universe involves mechanisms of baryosynthesis that generate an asymmetry from an initially baryon-symmetric Universe [8]. This theory is not yet supported by experimental evidence: neither baryon non-conservation nor large levels of CP-violation, both a required ingredient for a baryon asymmetry, have been observed. The detection of antinuclei with $A>3$ would hint to the existence of residual antimatter from the Big-Bang nucleosynthesis, while heavier particles such as anti-carbon will hint to the existence of stellar nucleosyntesis in antimatter domains or lumps of antimatter [9].

ALADINO will achieve the first experimental detection of antinuclei in the cosmic radiation.

2.2 Dark matter

While no evidence for DM particles has been found in experiments at the Large Hadron Collider, the TeV-scale DM models are nicely supported by cosmological requirements. The thermal freeze-out mechanism of weakly interacting O(TeV)-massive particles can provide quite naturally the required level of abundance of cosmological DM in today's Universe inferred by cosmological observations. Such large predicted mass for the DM candidate makes its production cross-sections at the LHC extremely suppressed [10] and even prospects for future colliders are not encouraging [12]. Their direct detection via elastic scattering off nuclei is also disfavored [11], while indirect search seems to be the most promising approach. In fact, there is a promising parameter space to explore for TeV-scale DM candidates consistent both with gamma-ray and the Cosmic Microwave Backgrounds limits [67] [13].

Elementary antiparticles such as positrons and antiprotons are well-known components of the cosmic radiation since their first detection in the sixties and late seventies, respectively. Since many years it has been known that these particles can shed light on the nature of the DM. In recent years, this field has witnessed significant advancements on both experimental and theoretical sides, pushed by new-generation experiments such as PAMELA, the Fermi-LAT telescope, or the Alpha Magnetic Spectrometer AMS-02. An unexpected rise was observed in the positron flux at energies above 10 GeV, in contrast to all secondary production calculations that predict a decreasing behavior in the GeV-TeV energy range. It suggests the existence of unknown sources. In the last years, hundreds of papers have proposed interpretations in order to explain the positron excess, either invoking annihilation/decay of DM particles or nearby astrophysical sources such as pulsars or supernova remnants [14].

Anisotropy studies on the arrival direction of high-energy particles may provide the complementary information needed for identifying the positron sources. High-energy leptons lose rapidly their energy while they travel in the ISM. Those detected at the highest energies must have been produced in the vicinity of the solar system (within ~1 kpc) in order to reach the Earth. Localized sources of CR positrons may be detected by anisotropy measurements, hence favoring or disfavoring particular models of sources.

By measuring energies and arrival directions of CR electrons and positrons at the TeV scale, ALADINO has the capability to clarify the origin of the anomaly in the positron fraction, assessing the possible contribution of nearby sources and the induced anisotropy

A more convincing DM signature would be an excess on antiprotons flux at high energies. Such a scenario is consistent with astrophysical γ-ray bounds and well theoretically motivated, especially considering the absence of new physics from LHC. To decide whether a DM signal is hidden, secondary production models need to be better constrained, and antiproton measurements extended above TeV.

ALADINO is well suited for investigating TeV scale DM models since it is specifically designed to probe the multi-TeV energy range of the positron and antiproton spectra.

Anti-deuterons represent a promising channel for DM searches: the astrophysical background is highly suppressed in the expected signal region for TeV DM models, therefore a null result on this channel search will have strong implication for a wide range of viable DM models. Conversely, a positive detection would represent the first observation of such particles in CR and will have a large impact also in understanding astrophysical processes.

ALADINO will be able to search for anti-deuterons with unprecedented sensitivity.

2.3 CR protons and nuclei

Recent direct measurements on primary protons and nuclei shed new light on acceleration and propagation mechanisms. The paradigm of a unique power law energy spectrum below the knee, down to the region where solar modulation effects become sizeable, might have been overcome.

ALADINO will extend the spectrometric precision to fully cover the break region and measuring very well the spectral indexes for individual nuclear species. Evidence for the observed hardenings could be checked and better quantified. This would be very important for a comparison with state-of-the-art models of galactic CR acceleration/propagation mechanisms, also studying the possibility of a contribution of nearby sources. Moreover, measurements of the ratio of secondary vs. primary cosmic rays will constrain the propagation models of CR in our galaxy.

Since the first experimental evidence [16], the energy region around the knee in the all-particle cosmic ray spectrum, at about 3 PeV, has been investigated by many experiments with different approaches. Several theoretical explanations have been proposed exploiting different hypotheses on source properties/populations, acceleration/propagation mechanisms and particle physics issues at high energies [17]. After the first results at the Large Hadron Collider (LHC), the ``particle physics'' origin of the knee is clearly disfavored, confirming that it is a genuine property of the CR spectrum itself [18]. It remains still unsolved whether the (dominant) origin of the knee is due to the reach of the maximum energy achievable at the sources or to diffusion processes in the Galaxy. In both cases a rigidity dependent sequence of knees in each single element spectrum is the most probable scenario [17]. For the analysis of the CR flux, direct measurements carried on space or stratospheric balloons actually give the best performance in terms of both energy resolution and charge identification. However, due to their limited acceptance and the steeply falling fluxes, they do not give clear information on the steepening of various elements nor on the knee of each species or of the all-particle spectrum itself.

Moreover, chemical composition is shown to evolve towards heavier nuclei, with helium becoming more abundant than hydrogen at energies of about 10-20 TeV [19]. It is then mandatory to explore the energy region up to few PeVs with high precision direct measurements to study the energy spectra of each individual nuclear species, to detect any possible hardening of the spectral indexes and to set mass composition below the knee of

the all-particle spectrum. A detection of the steepening of each single species and then the explanation of the all-particle knee would be a crucial result in understanding galactic CR physics, also serving as fundamental input to the study of the extra-galactic component.

ALADINO will give high precision direct determination of CR proton and nuclei spectral indexes below the knee and will provide the first direct measurement of the all particle spectrum up to the knee. The p and He component will be measured up to PeV, allowing the first direct measurement of the maximum energy provided by the CR sources.

2.4 CR transport in the heliosphere

Measurements of low energy CR flux variation with time will allow gaining a deep understanding on CR transport in the heliosphere on monthly, weekly, or even daily basis. Data can be compared with the missions that have or continue to collect data related to the heliosphere including the Solar Anomalous and Magnetospheric Particle Explorer, the Solar and Heliospheric Observatory, the Solar Dynamics Observatory and others. Moreover, the comparison with Voyager data taken outside of the heliosphere will allow precisely determining the CR Local Interstellar Spectrum.

With its unprecedented sensitivity, ALADINO will allow high precision measurements of the heliosphere influence on CR fluxes.

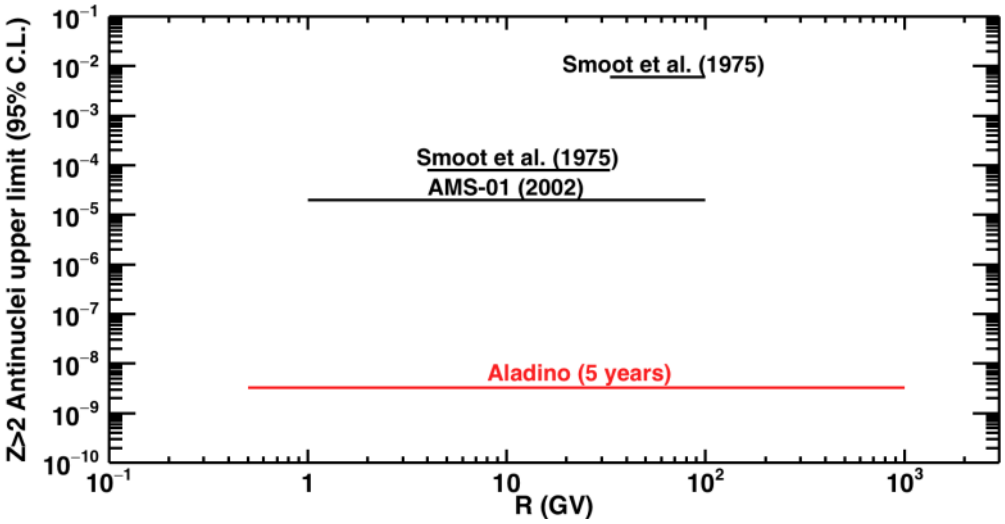

Figure 1. *Current experimental limits for heavy antimatter search [73, 74] and the expected ALADINO reach.*

3 SCIENTIFIC REQUIREMENTS

The accomplishment of the ALADINO science goals is subjected to the verification of measurement requirements which are discussed in this section. Orbital conditions and operational requirements are discussed later in this proposal (section 5).

The instrument must be capable to collect electrically charged particles with the ability to discriminate between particles and antiparticles over unexplored energies and

with higher sensitivities with respect to present experiments. Discrimination between leptons and hadrons, nuclear charge measurements, and mass separation will provide complete particle identification. The key physical quantities characterizing the basic properties of CR particles are: charge magnitude and charge sign, incoming direction, velocity, momentum and/or total energy. An important performance parameter is the *collection factor* (in units of m^2 sr yrs), representing the product between exposure time and total acceptance over a given energy range. Measurement requirements are outlined in the following, where the ALADINO physics targets are factorized into specific observational goals.

3.1 Nuclear Antimatter

The detection of heavy antinuclei ($|Z|= 3 - 8$) or anti-helium would have strong implications for Cosmology. The best experimental limit on the antihelium/helium flux ratio is set as 10^{-8} in a very limited rigidity range (1.6-14 GV) by the BESS experiment [6], in a wider interval (0.6-600 GV) the PAMELA spectrometer has achieved the next to best limit as of 2.67 10^{-7} [20]. The goal of ALADINO is to improve the current limits of a 10^3 factor at least, this implies the identification of one antihelium out of 10^{11} Z=2 particles. Production of anti-helium can be foreseen also in some DM scenario or, although strongly suppressed, in the collision of CR with the ISM as discussed later in section 3.2, under these hypotheses, the ALADINO sensitivity will allow the first detection of such a signal.

For heavier antinuclei, the current observational limits, shown in Figure 1 will be improved at least of 4 orders of magnitude.

ALADINO goal is to extend the current observational limits for helium and heavy antinuclei by at least 3 and 4 orders of magnitude respectively, which translates into a collection factor of ~15 m^2 sr yr

3.2 Dark Matter

3.2.1 POSITRON SPECTRUM

Figure *2* shows a recent groundbreaking result on the positron fraction $e^+/(e^+ + e^-)$ first measured by PAMELA [21] and later confirmed by Fermi-LAT [22] and AMS-02 [23]. Some popular candidate DM particle models that may explain the data are also shown in the figure. The high-energy DM signal well exceeds the astrophysical background of secondary species, and all interpretations point consistently toward DM masses in the TeV range, i.e., significantly higher than those expected just a few years ago.

Along with DM models, various astrophysical mechanisms have been proposed to explain the excess [14][15]. Proton-proton collisions taking place in the shockwaves of supernovae remnants could produce a source component of high-energy positrons, accelerated with a hard spectrum, therefore producing a rising positron fraction. Positron and electron pairs may also be produced and accelerated inside the magnetosphere of

nearby pulsars. An example of the latter scenario is given in Figure 1d, showing that pulsar models can describe very well the observations. Models proposing significant modifications in the environment of CR sources or in CR propagation have been also put forward to interpret the anomaly.

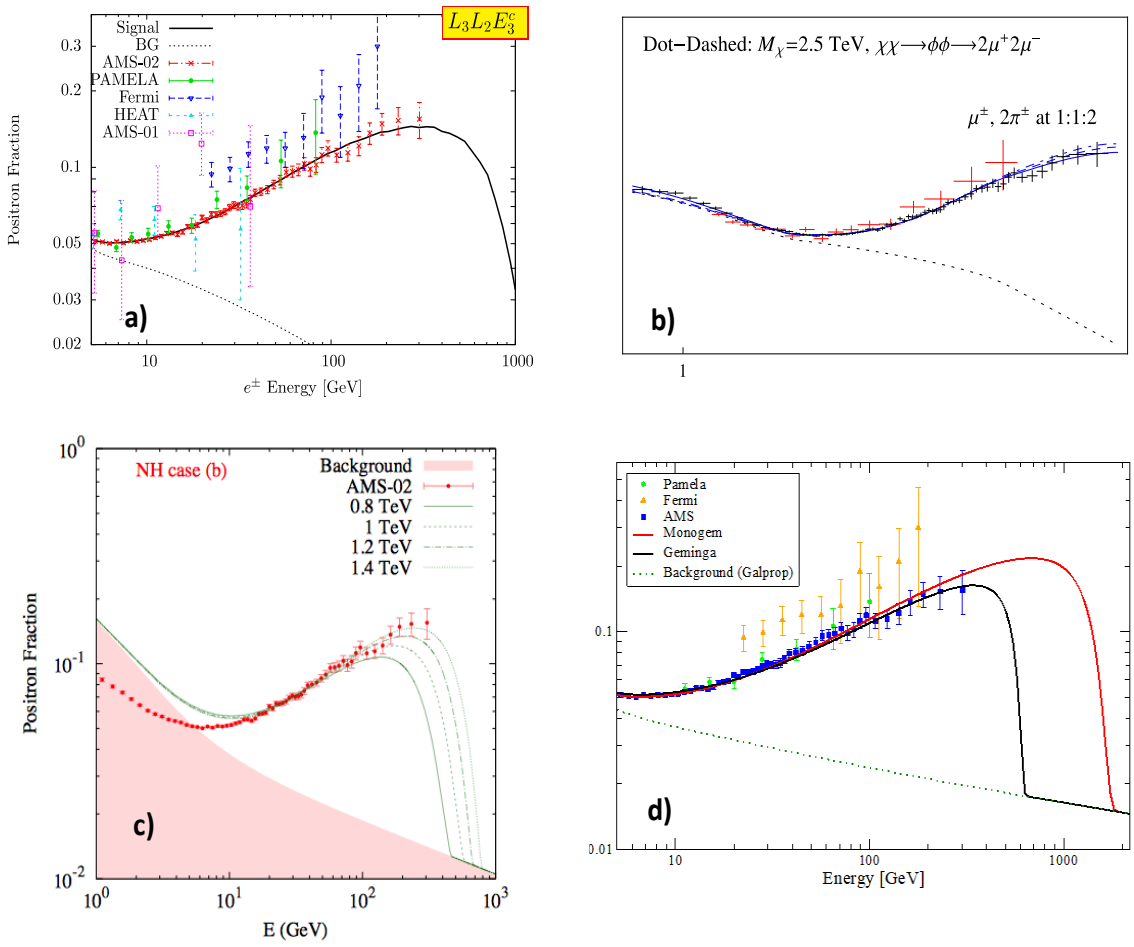

Figure 2. *The measured positron fraction as a function of positron energy compared with various DM models. (a) decay of a wino-like neutralino of mass 3 TeV [27]; (b) DM particles with mass of ~1-3 TeV annihilating to intermediate states that then decay to muons or charged pions [28]; (c) a scalar multiplet extension of the SM accommodating non-zero neutrino masses [29]; (d) contributions from Geminga (black) and Monogem (red) pulsars [30]. The decreasing astrophysical background is shown for reference in all plots*

An important signature of the different scenarios consists in different cutoff values for the energy spectra of electrons and positrons (and in the fraction) in the 200 GeV – multi-TeV energy region. At energies above AMS-02 reach, few of these predictions are being tested by ongoing experiments CALET [24], DAMPE [25], and the forthcoming ISS-CREAM experiment [26].

However, the ability of these experiments to settle the issue once and for all is plagued by the absence of antimatter identification capability. Moreover, it is questionable that it will be possible to resolutely discriminate between pulsar and DM sources by only

measuring $e^{+/-}$ energy spectra, because both scenarios have large numbers of unknowns (i.e. free parameters) and no a priori prescription.

However the precise measurement (at the percent level up to TeV region) of the electron and positron fluxes) should restrict dramatically the parameter space region of DM or pulsar unknowns. Combining these constraints with other astrophysical observations (pulsar models) or accelerator data (DM) and/or anisotropy measurement will provide an important improvement in the study of the origin of the excess.

ALADINO goal is to extend the measurement of electrons and positrons up to ~5 TeV of energy, which translates into a collection factor of ~15 m^2 sr yr. A lepton/hadron separation factor of ~10^6 is essential to avoid proton contamination. Misidentification of electrons as positrons due to charge confusion must be kept below 10^{-2} at all energies to prevent electron-induced background.

3.2.2 POSITRON ANISOTROPY

The current upper bound on positron anisotropy is set by AMS-02 at 3% [31][32]. Considering that predicted anisotropies from nearby pulsars range from a few percent to a few per mille or less, it is doubtful if AMS-02 will be capable of providing conclusive information even after 10 more years of observations. On the other hand, ALADINO, with two orders of magnitude larger acceptance and capable to measure the positron spectrum up to ~5 TeV, will be able to clarify if and which nearby astrophysical objects are sources of CR electrons or positrons, and if they contribute differently to the two components.

ALADINO observational goal is to reach a level of a few ~10^{-3} in the dipole anisotropy amplitude using CR positrons, which is where signatures of nearby CR accelerators would appear (see Sec.1). The current upper bound is set by AMS-02 at 3%. The essential requirement is to ensure a cumulated statistical sample of ~15 m^2 sr yr at E>100 GeV. An angular resolution of ~0.1 degree will guarantee the desired level of precision in the determination of the CR arrival directions. Full sky coverage is also required.

ALADINO goal is to measure the positron anisotropy amplitude at the ~$3 \cdot 10^{-3}$ level, which translates in a collection factor of 15 m^2 sr yr.

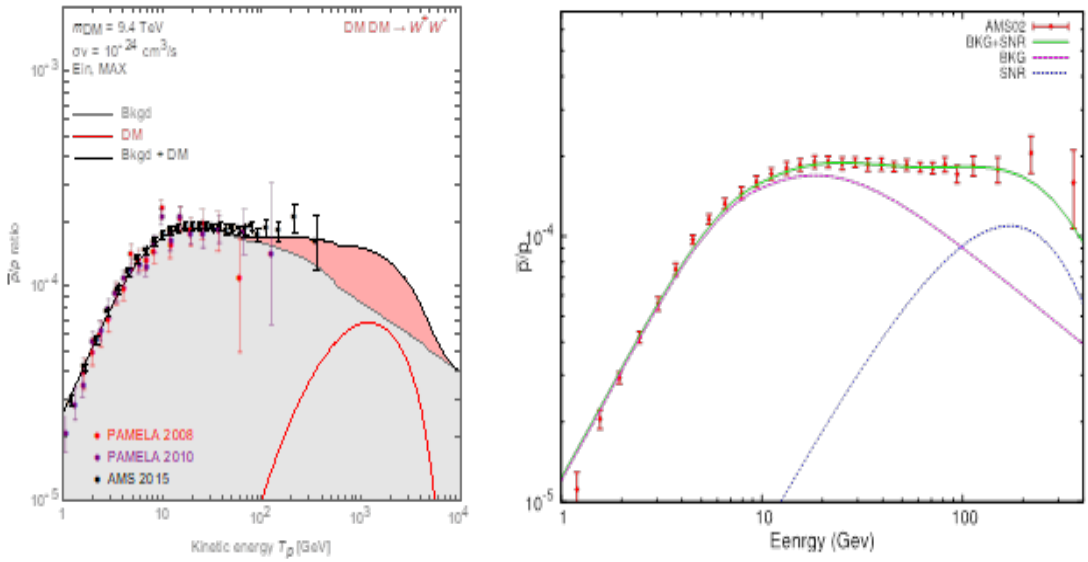

Figure 3. *Left: the measured antiproton-to-proton ratio as a function of energy compared to a theoretical model (black line) including the expected secondary antiproton component (grey line) and a 9.4 TeV Minimal Dark Matter quintuplet [33] [private communication] annihilating in W^+W^- (red line). Right: antiproton-to-proton data described in term of secondary components (purple) and a components arising from hadronic production inside supernova remnants (blue) [34].*

3.2.3 *ANTIPROTON SPECTRUM*

In contrast to positrons, antiproton data in the 1-100 GeV energy range do not show striking evidences of an excess over expected astrophysical background. Nonetheless, the AMS-02 experiment has very recently reported a remarkably hard antiproton flux (i.e., a flat antiproton/proton ratio) at energies up to E~450 GeV, which appears at tension with current models of secondary production [35][75].

Although these estimates are known to suffer from large uncertainties, the intriguing gap between the new AMS-02 data and the predicted background leaves room for DM annihilation contributions. As an example, Figure *3* (left) shows the predicted signal by a 9.4 TeV DM particle annihilating into a W^+W^- pair [33]. It is interesting to note that pulsar scenarios for the positron fraction do not predict any excess in the antiproton flux. A possible astrophysical explanation, however, may involve the hadronic production of antiprotons inside supernova remnants, from collisions of accelerated protons. An example of this model is given in Figure *3* (right). Besides the high-energy region of the antiparticle spectra, the significance of the low energy data should not be downplayed. Precise antiproton measurements at energies of 0.1-5 GeV allow probing DM models with ~10 GeV masses, to impose limits on primordial black hole evaporation or to produce novel constraints on CR propagation models. ALADINO measurements will overlap with AMS-02 or PAMELA data and with the data that might come from the

proposed balloon project GAPS [36]. Thanks to its large acceptance and orbit, over 5 years of data taking, ALADINO will provide a more than two orders of magnitude increase in the existing antiproton statistics in the energy range 100 MeV-5 GeV.

ALADINO goal is to extend of at least one decade in energy the antiproton flux measurement to test the TeV-scale masses DM annihilation models. To achieve this goal, a collection factor of ~15 m^2 sr yr is needed. A rejection factor of ~10^5 against mis-identified protons must be ensured. To avoid electron contamination, a lepton/hadron separation factor of ~10^4 is sufficient.

It is interesting to note that pulsar scenarios for the positron fraction do not predict any excess in the antiproton flux. A possible astrophysical explanation, however, may involve the hadronic production of antiprotons inside supernova remnants, from collisions of accelerated protons. An example of this model is given in Fig. 2 (right). Besides the high-energy region of the antiparticle spectra, the significance of the low energy data should not be downplayed. Precise antiproton measurements at energies of 0.1-5 GeV allow probing DM models with ~10 GeV masses, to impose limits on primordial black hole evaporation or to produce novel constraints on CR propagation models. ALADINO measurements will overlap with AMS-02 or PAMELA data and with the data that might come from the proposed balloon project GAPS [36]. Thanks to its large acceptance and orbit, over 5 years of data taking, ALADINO will provide a more than two orders of magnitude increase in the existing antiproton statistics in the energy range 100 MeV-5 GeV.

3.2.4 ANTIDEUTERIUM AND ANTIHELIUM SPECTRA

In contrast to antiprotons, which suffer from large astrophysical background, complementary searches with antideuteron or antihelium nuclei would benefit from promising DM signals [37] [38] and strongly suppressed background in the expected signal region (due to the kinematics of antinuclei production in proton+ISM or helium+ISM collisions), thereby offering a potential breakthrough for new physics discoveries [76]. Consequently, a null result on the detection of these particles will have strong implications for a wide range of viable DM models.

Figure *4* (left) shows the predicted antideuteron flux as a function of kinetic energy per nucleon for various DM models and secondary production along with current upper limits and secondary background calculations. ALADINO, with a predicted sensitivity in 5 years of ~$3 \cdot 10^{-8}$ part/(m^2 sr s GeV/n) at the 95% C.L in the 0.1-0.8 GeV/n kinetic energy region, will probe many viable models of light and heavy DM particles. The sensitivity reached in the antihelium/helium ratio is illustrated in Figure *4* (right).

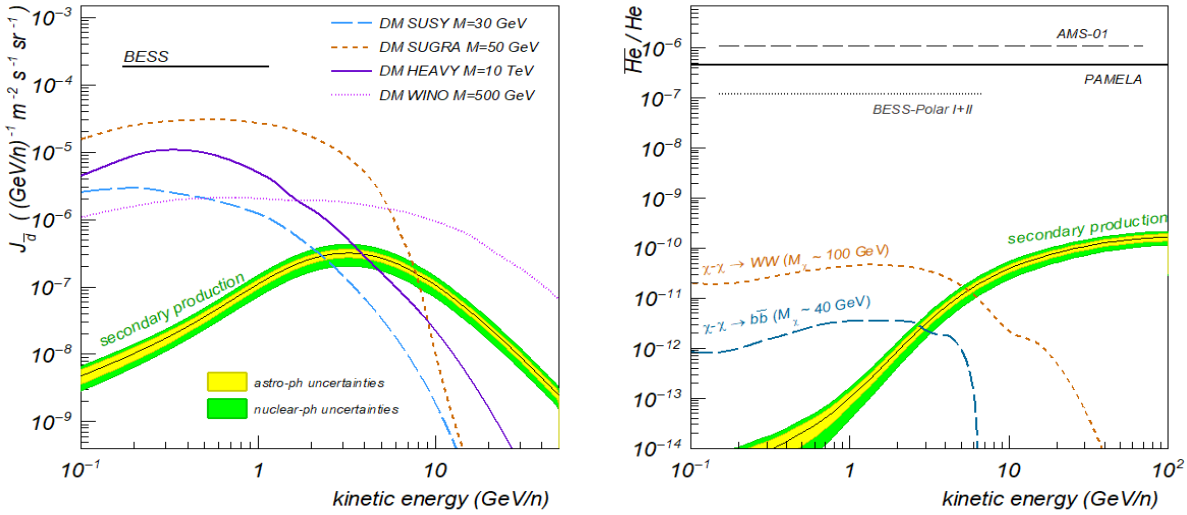

Figure 4. *Antideuteron flux (left) and antihelium/helium flux ratio (right) as a function of kinetic energy per nucleon expected by secondary production and various DM scenarios [36][37][38]. Upper limits from BESS [39], PAMELA [20] and AMS-01 [23] are shown. Red lines report the expected ALADINO sensitivities. The expected AMS-02 sensitivity in 10 years are ~10^{-9} part/(m^2sr s GeV/n) for antideuteron at E=0.1-1 GeV/n, and ~10^{-9} for antihelium/helium ratio at 0.1-50 GeV/n.*

3.3 High energy CR (electrons, protons and nuclei)

3.3.1 HIGH ENERGY ELECTRONS

As stated before, the electron/positron component of CR, because of the low mass, suffers significant energy losses during the propagation in the Galaxy. Such large losses produce a steeper energy spectrum compared to that of protons and actually place upper limits on the age and distance (at about 10^5 yr and 1kpc, respectively) of the astrophysical sources of high-energy electrons. Since the number of such nearby objects is limited, the electron energy spectrum above few TeV is then expected to exhibit spectral features, and a sizeable anisotropy in the arrival directions is also foreseen at very high energies [41]. In this context, the multi-TeV, largely unexplored, region is very interesting because of the high potential for studying local sources. Indirect measurements made by imaging atmospheric Cherenkov telescopes suggest, even with large uncertainties, a cutoff at about 1 TeV [42]. The exploration of the high-energy part of the spectrum with high precision direct measurements is then mandatory. This can be afforded by ALADINO thanks to its large MDR spectrometer and high precision large acceptance calorimeter with suitable tracking section and ion charge measurements, in order to have a sufficient discrimination against primary protons and nuclei. Up to 10 TeV measurement of e^- component of the flux will be possible thanks to the large MDR of the spectrometer and the absence of e+ background. At higher energies the calorimetric measurement of the “all-electron” (e^- + e^+) flux, will be performed.

The all-electron flux is measured from GeV to TeV energies by several direct detection experiments, which reported large discrepancies each other (factor ~2). The recent AMS-02 data reached a precision below ~10% at E< 1 TeV. The spectrum at E~1-10 TeV has been measured by only indirect detection techniques that suffer from large systematics. The H.E.S.S. observatory has reported a cut-off of the flux at E~1-2 TeV. Possible signatures of nearby sources of CR leptons may appear in the spectrum at about E ~10 TeV. The ALADINO physics goal is to measure the all-electron spectrum from 0.5 GeV to nearly ~50 TeV of energy, with a statistical precision of a ~2% at E~1 TeV. The multi-TeV flux measurement demands collection factor of ~20 m^2 sr yrs. To detect flux variations in this energy region, the resolution δE/E of the instrument should be ~5% at E>1TeV. To control the dominant proton-induced background, the lepton/hadron separation capability must approach the level of 10^6.

The ALADINO calorimetric measurement of the all-electron energy spectrum, after few years of operation, is shown in Figure 5.

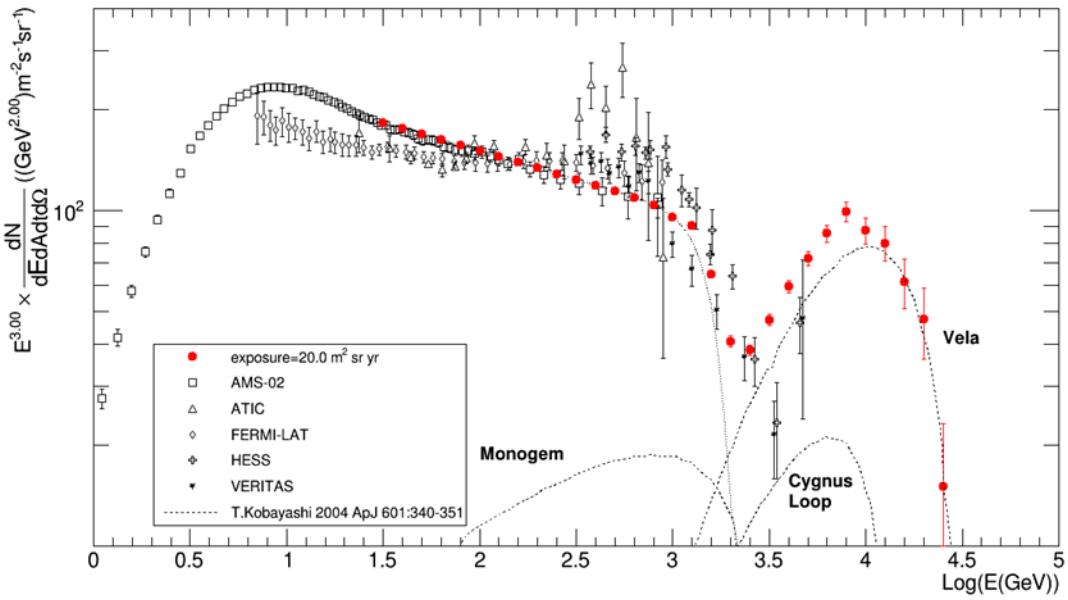

Figure 5. Calorimetric measurement of the all-electron energy spectrum done by ALADINO with a 20 m^2 sr yr exposure (see text for details).

The input spectrum was simulated by assuming a power law with a spectral index as given by AMS-02 [40] data above 30 GeV, a cutoff at about 1 TeV as suggested by HESS and VERITAS in [42][43], and then a possible contribution of three nearby sources as parametrized in [41]. In the figure, the result is compared with AMS-02, ATIC, FERMI-LAT, HESS and VERITAS measurements and with the model given in [41]. As can be seen, this will allow a direct and precise detection of the possible cutoff at about 1TeV. Moreover further structures/excesses due to nearby sources would be clearly identified up to about 30 TeV, together with possible indirect evidence for a DM-induced

excess. In the case of sizeable contribution of nearby sources, a large anisotropy is also expected at high energy, which could be easily detected by ALADINO, giving important clues to the understanding of diffusion processes in the Galaxy. ALADINO goal is to extend the calorimetric measurement of all electrons up to ~50 TeV of energy which translates into a collection factor of ~20 m^2 sr yrs.

3.3.2 CR PROTONS AND NUCLEI FROM 100 GEV/n UP TO 50 TEV/n

In 2010 the CREAM (Cosmic Ray Energetics And Mass) experiment showed evidence for the hardening of the proton and of the nuclei spectra with different ("discrepant"') spectral index changes. This is summarised in Figure 6 (upper panel) where CREAM data, also fitted by (broken) power laws, are shown together with other measurements [44]. Even with large error bars (mainly at high energy and/or for heavier primaries), a change of spectral index is suggested at about 200 GeV/n. Both the energy ranges and the flux uncertainties prevented anyway a clear claim for a break in the proton and helium spectra.

This has been possible after the analysis of PAMELA results, later confirmed by AMS-02. As can be seen in the lower panel of Figure *6*, a clear change of spectral index is shown by data, even if different experiments give slightly different slopes after the breaks. More data are then needed at high energy in order to measure, with a single experiment, the region across the breaks with small uncertainty. A precision spectrometric measurement up to 20 TeV with a collection factor of 15 m^2sr will allow fully covering the energy region of the breaks and accurately determining the change in the spectral indexes. At higher energies, calorimetric measurement will take over due to its larger acceptance. No critical background is expected provided that a charge resolution of $\delta Z \sim 0.2$ is achieved. Common sources of systematic errors are related to the assessment of the absolute scale for energy and momentum and their resolutions, minimized thanks to the simultaneous rigidity/energy measurement in a wide interval.

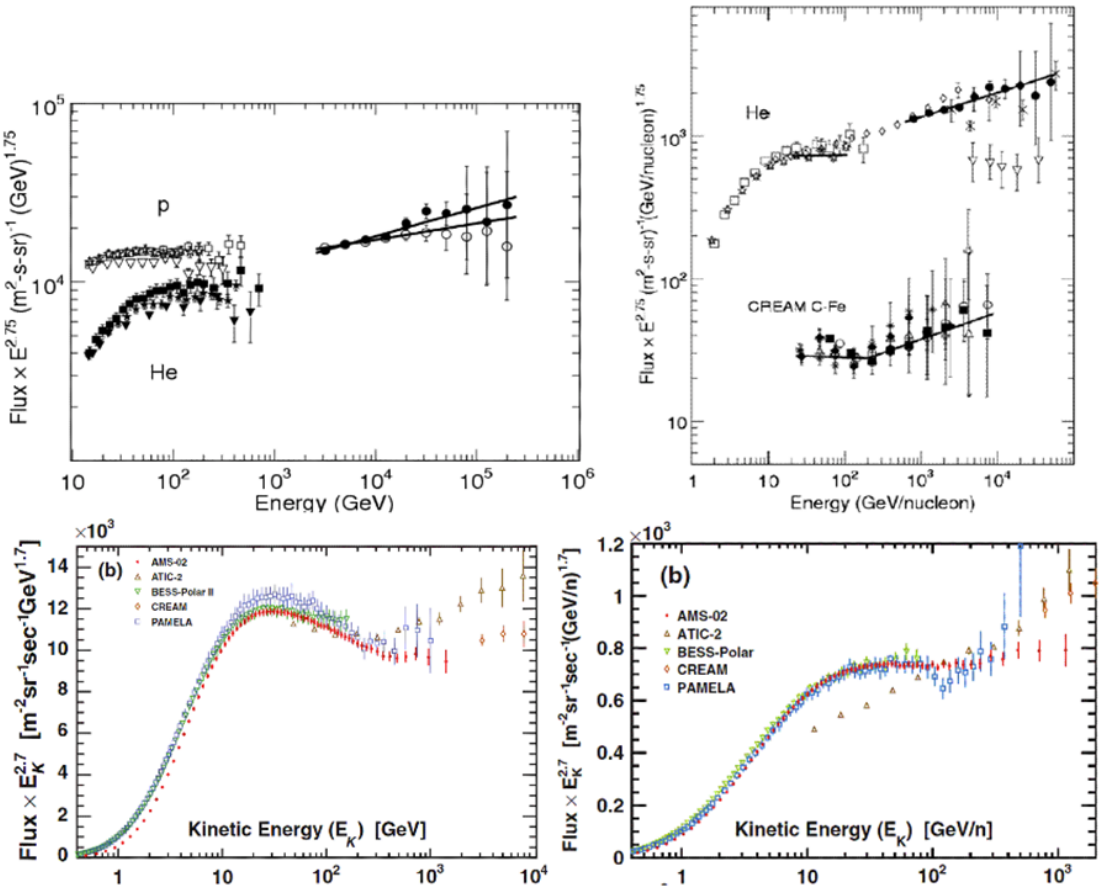

Figure 5. *Upper panel - Measurements of proton, helium and nuclei fluxes as for year 2010: first evidence for discrepant hardenings by the CREAM experiment [44]. Lower panel - Recent measurements on proton and helium fluxes (left and right plots respectively) by the AMS-02 experiment [45].*

Measurements of primary (C-N-O) and especially secondary (Li-Be-B) nuclei in the currently unexplored ~1-50 TeV/n energy range will provide an essential input for estimating the astrophysical background for DM signals. This will also provide an essential input for understanding the origin of the hardening of the CR spectra since different models (where the hardening can originates in the CR source or during the CR propagation) do not predict the same hardening amplitude for primaries and secondaries.

This measurement is subjected to the same requirements of protons, plus a charge separation capability of $\delta Z \sim 0.15$ for all elements. A further requirement is to address the background generated by charge-changing fragmentation processes occurring in the detector material. These issues can be addressed by multiple charge measurements operated at different levels of the apparatus. The improvement in current measurements of B/C flux ratio with ALADINO 20 m^2 sr yr exposure is shown in Figure *7*.

ALADINO aims to accurately measure nuclear fluxes up to 50 TeV/n energies will be possible thanks to the large calorimetric acceptance and the redundant measurements of particle charge given by ToF and Tracker. A collection factor of 20 m^2 sr yr will be needed for the measurement of 2<Z<8 species.

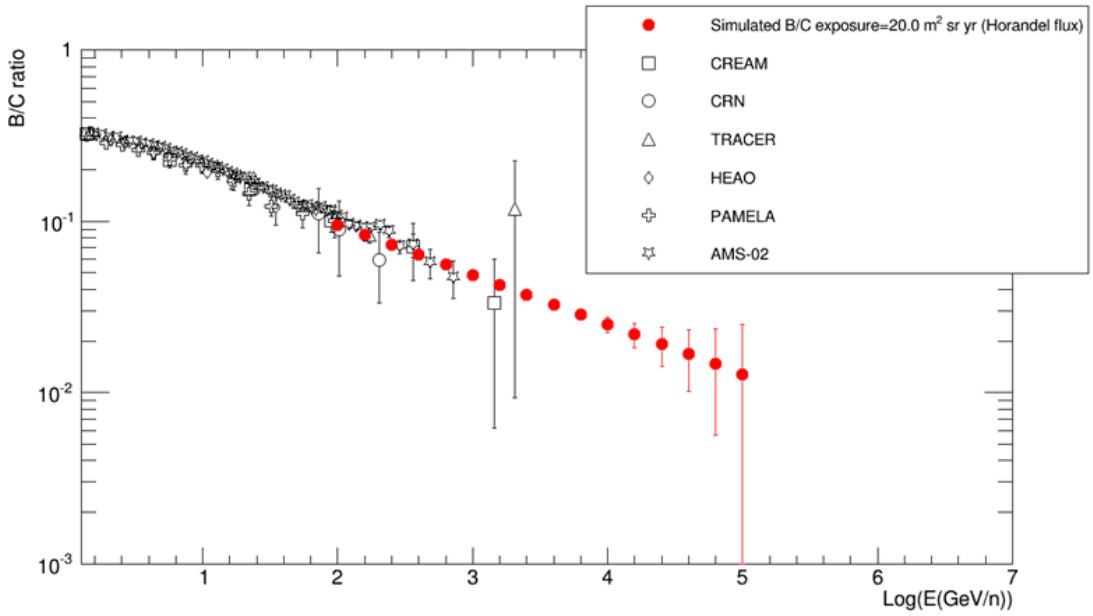

Figure 6. *Simulated B/C flux ratio calorimetric measurement with ALADINO for a 20m^2 sr yrs exposure.*

3.3.3 REACHING THE ALL-PARTICLE KNEE

Direct measurements carried on space or stratospheric balloons could hardly reach, up to now, energies of hundreds of TeV due to their limited acceptance/exposure, then no direct clear information exists neither on the steepening of various elements nor on the knee of each species or of the all-particle spectrum. Conversely, ground based experiments – measuring CR from the characteristics of their showers in atmosphere – have larger exposures but are affected by large systematic errors related to the energy scale uncertainty and the dependence of particle identification (Z) from the shower modeling. Current missions like CALET and DAMPE (and the planned ISS-CREAM experiment) will extend high-energy measurements up to about 100 TeV, but will hardly reach the interesting region of the knees for each different species. A collection factor of 20 m^2 sr yr and charge measurement with a $\delta Z \approx 2$ are needed to extend p and He measurements at the PeV energies. Simulated ALADINO results for the measurement of protons and nuclei, after an exposure of 20 m^2 sr yr, obtained by assuming flux parameterization as given in [46], are shown in Figure *8*. ALADINO points (in color) are compared with measurements from PAMELA, CREAM, AMS-02 and ATIC experiments (in black) and theoretical models [46] [47]. Proton and helium component are measured

up to PeV energies, thus allowing to get the first direct evidence of the light component knee, corresponding to the maximum energy provided by the CR source(s).

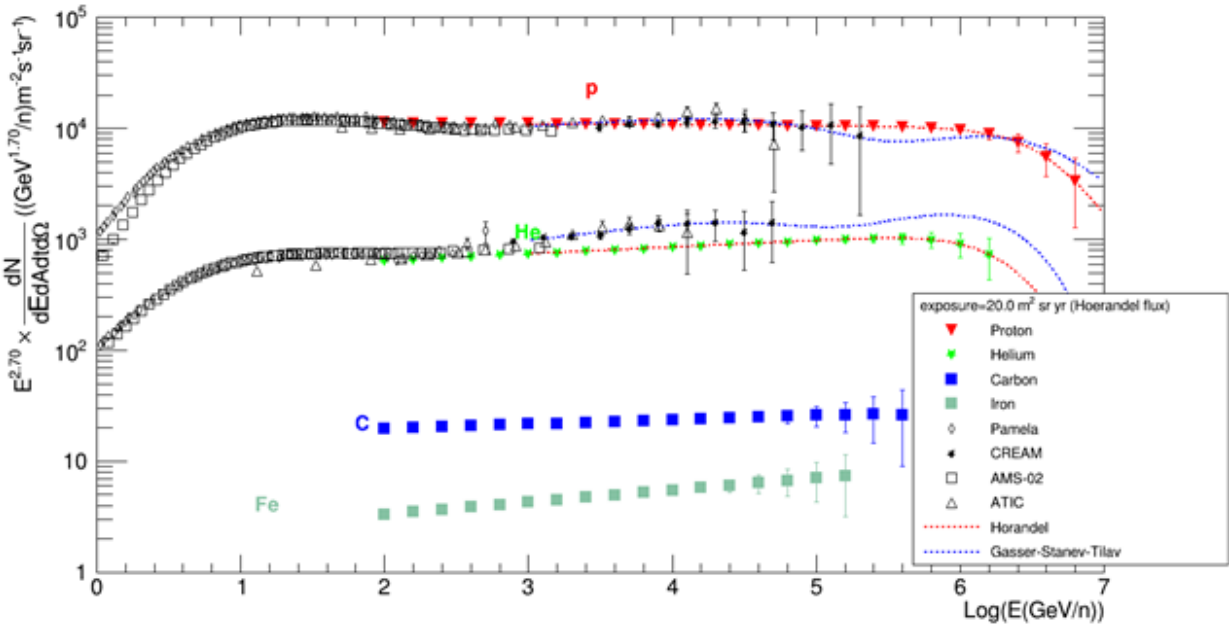

Figure 7. *Contribution of the ALADINO mission after few years of operation (20 m^2sr yr) to the measurement of individual proton and nuclei energy spectra.*

ALADINO goal is to measure proton and He fluxes in the energy range E=0.5 GeV/n – 1 PeV/n, which translates into a collection factor ≥20 m^2 sr yr.

3.4 CR transport in the heliosphere

The study of long-term solar modulation demands an acceptance of at least ~0.5 m^2 sr, in the ~0.1-50 GeV/n energy range, in order to perform a CR flux reconstruction over monthly, weekly, or even daily basis. The stability of the detector performance with time is important for this investigation.

ALADINO goal is to measure p and He daily fluxes in the energy range 0.5-50 GeV/n, which translates in an acceptance of 0.5 m^2 sr.

4 MEASUREMENT CONCEPT

The ALADINO payload comprises all the three key elements needed to satisfy the measurement requirements for the proposed science theme:

1. a superconducting magnetic spectrometer to measure the particle rigidity, charge magnitude and sign, with a maximum detectable rigidity exceeding 20 TV and an acceptance of 3 m^2sr;

2. a Time of Flight (ToF) system to measure the particle velocity and charge magnitude;
3. a large acceptance (≈9 m^2sr) 3D imaging calorimeter to measure particle energy and discriminate electromagnetic ($e^{\pm}$) from hadronic ($p^{\pm}$) components.

The ToF and the calorimeter also provide signals to trigger the start of data acquisition on minimum ionizing and showering particles respectively.

These elements are incorporated in the cutting edge design presented in Figure *9*, which maximizes the acceptance while keeping the overall payload size, a cylinder of 440 cm in diameter and 200 cm in length, within the fairing volume of an Ariane 5 class launcher. This design fully exploits the isotropy of the cosmic-ray flux up to very high energies: orbiting with its axis pointing towards the zenith, particles are collected over a wide solid angle on the lateral surface of the cylinder. The axial symmetric configuration of the detectors guarantees a uniform efficiency in the response of detectors regardless of the particles' arrival direction.

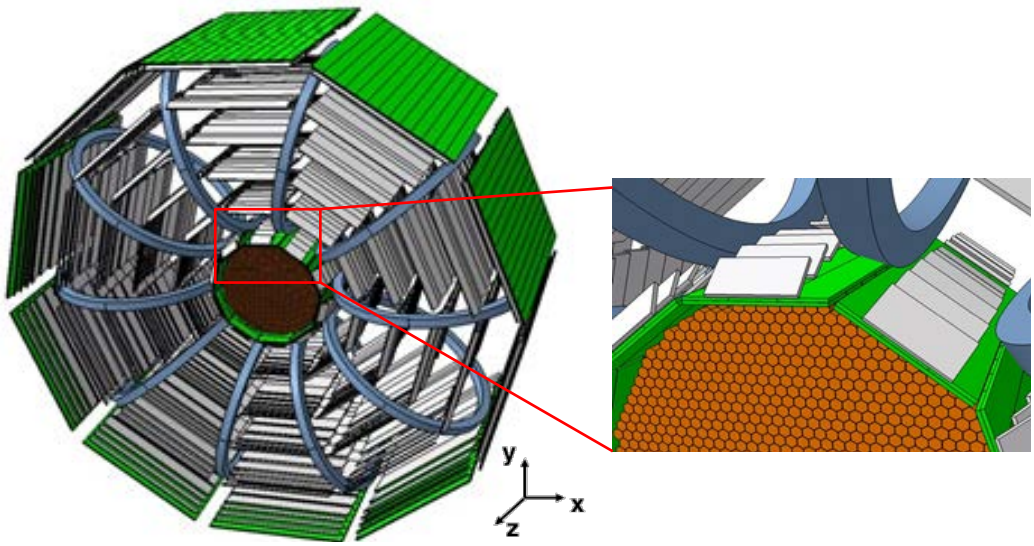

Figure 8. Left*: overview of the ALADINO detector. The core of the apparatus is the cylindrical calorimeter, represented in orange. The ten circular magnetic coils surrounding the calorimeter are sketched in blue. The silicon micro-strip tracking system, arranged in six layers, is composed of several ladders drawn in gray. The ToF layers, segmented in paddles, are represented in green. The internal ToF layers are barely visible between the calorimeter and the first layer of tracker.* Right*: detail of the central part of the apparatus; the segmentation of the calorimeter in (xy) view is clearly visible, as well as the ToF inner layers placed between the calorimeter surface and the first tracker layer. Sensors in the tracker are oriented such as to maximize the resolution.*

Two innovative techniques enable this advanced design:

1. the use of a superconducting magnet based on a high temperature lightweight superconductor material developed for space application within the EU-FP7 SR2S project[55]. This allows to reach an intense magnetic field, average 0.8 T, over the large volume of the spectrometer. In conjunction with the precise tracking of silicon detectors, this results into a maximum detectable rigidity of the spectrometer exceeding 20 TV;
2. based on the CaloCube R&D project [49], the cylindrical calorimeter is made of a 3D mesh of small hexagonal prism-shaped scintillating LYSO crystals: it insures a nearly isotropic response to particles entering from different directions thus maximizing the detector acceptance. The highly segmented design allows for reconstructing the shower development inside the calorimeter so as to provide the required $e^{\pm}/p^{\pm}$ discrimination besides measuring of the energy released by the interacting particle.

The ToF and silicon tracker detectors are based on the successful design used in AMS [50][51] and PAMELA experiment [52].

The main characteristics of the ALADINO experiment are summarized in Table 1. A detailed description of the different subsystems is presented in the following sections.

Table 1: *main performance parameters of the ALADINO apparatus*

Calorimeter acceptance	~ 9 m^2 sr
Spectrometer acceptance	~ 3 m^2 sr
Spectrometer Maximum Detectable Rigidity	> 20 TV
Calorimeter energy resolution	24% ÷ 35% (for nuclei) 2% (for electrons and positrons)
Calorimeter e/p rejection power	> 10^5
Time of Flight measurement resolution	180 ps

4.1 Calorimeter: description and performances

A 3D mesh of 15925 small LYSO scintillating crystals arranged to form a nearly regular cylinder constitutes the calorimeter as shown in Figure 10. The front view of the calorimeter inside the ALADINO experiment is shown in Figure 9.

The chosen geometry is the most effective compromise between a fully isotropic calorimeter, i.e. a sphere with uniform response to particles over its entire surface, and the need to use part of the field of view to locate electronics/mechanical structures and services for the payload. Adjacent crystals are separated by gaps to both increase the

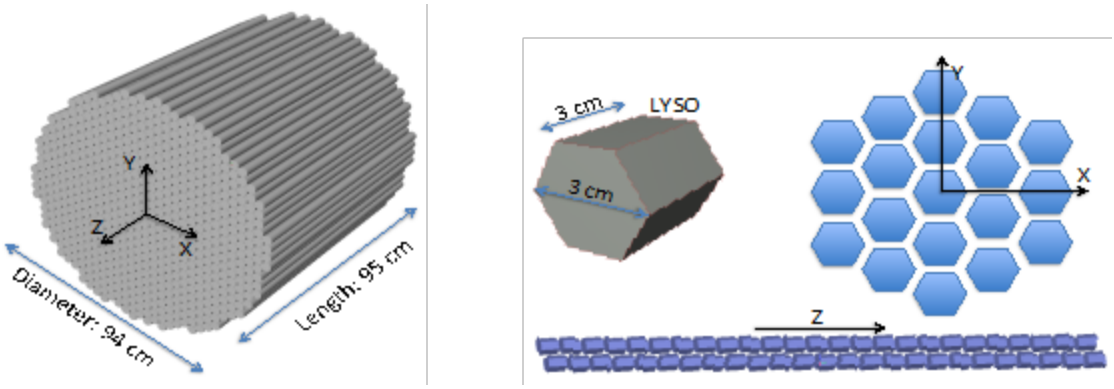

Figure 9. *Upper, from left to right: the overall assembly of the hexagonal-prism-shape crystals – a total of 15925 elements are foreseen, arranged in 637 lines, each composed by 25 crystals; design of the basic crystal; an example of 19 assembled crystals on the X-Y plane – a 8 mm gap among the crystals allows to accommodate the support structure and, possibly, the read-out system. Lower: design of two adjacent strings of 25*

overall detector volume, thus maximizing its acceptance at equal mass, and to accommodate support structures for single crystals and readout elements.

Single elements are shaped as 3 cm height regular hexagonal prisms and disposed such as to completely avoid escape planes, i.e. particle trajectories completely sneaking in between the calorimeter gaps. This is particularly relevant for energy resolution. Since the typical width of the electromagnetic shower component is quite narrow, the presence of escape planes would increase the event-by-event fluctuations in the total energy deposit, worsening the energy resolution. Thanks to the adopted geometry, relatively large gaps, 8 mm, can be then left between crystals increasing the total acceptance without a significant loss of energy resolution.

The crystals are made of Cerium-doped Lutetium Yttrium Orthosilicate (LYSO). LYSO is a dense, bright inorganic scintillator, which is nowadays commercially available, being industrially produced by several companies for high-precision Positron-Emission Tomography. Its density (ρ=7.4 g cm^{-3}), radiation length (X_0=1.14cm), Molière radius (R_M=2.07 cm), nuclear interaction length (λ_I =20.9cm) and refractive index (n=1.82) make it a competitive material for compact calorimeters. Its emission is centered at 430 nm, with a decay time constant of 40 ns; it is rather insensitive to temperature changes (dLy/dT (20 °C) = − 0.2% per °C) and thus suitable for high-precision calorimetry in the harsh space environment.

Following the design of Figure 10, the calorimeter depth along the diameter corresponds to 3.5 λ_I or to 61 X_0. Its total weight is 2000 kg with a 8.93 m^2sr geometric factor of the lateral surface.

Signals in the calorimeter crystals may vary from the ≈ 50 MeV released by Minimum Ionizing Particles (MIP), i.e. relativistic protons not interacting in the detector, to the 10^7 MIP signal released in one single crystal by a PeV interacting hadron. A correspondently wide dynamic range is then required for their readout.

The light produced in the calorimeter can be measured by photodiodes glued directly on the surface of each crystal. Two different photodiodes, one with a large collecting area for low signal intensities and one of smaller area for high intensity signals, coupled to a large dynamic range front-end electronics can be used to match the required dynamic range. This approach, tested within the CaloCube project partially suffers from the ionization signal directly produced by particles traversing the photodiode.

In ALADINO an alternative solution has been studied, which uses wavelength shifting (WLS) fibre bundles coupled to the faces of the crystals, bringing the light signals to photo sensors (e.g. Silicon Photo Multipliers or MAPMT) installed outside the active volume of the calorimeter. Moving from one prism to another, along a string, the fibre bundles are arranged on consecutive sides. In order to cover the requested high dynamic range each scintillator crystal could be read-out by two different sensors, each one receiving a different fraction of the collected light. The optimization of the number, size and arrangement of the fibres is an essential issue to be addressed during the realization of the project. A conceptual design is shown in Figure 11.

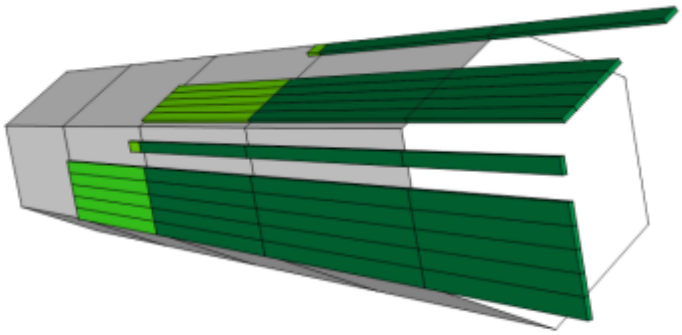

Figure 10. *layout of a possible arrangement of the WLS fibres in order to ensure a dual read-out with different dynamic range capabilities. Light green identifies the fibre portion in optical contact with the crystal scintillator. A different number of fibres, with longer or shorter optical contacts to the crystal, feed photo-sensors devoted to the readout of low or high intensity signals.*

The calorimeter performances have been studied using the GEANT package [52][53]. The full geometry was implemented, including the carbon fibre support structure in between crystals. Isotropic fluxes of electrons and protons at 1 TeV have been

simulated on the cylindrical surface. Thanks to the 3D segmentation of the calorimeter volume, a reliable shower image reconstruction is possible allowing to estimate the length of the shower inside the calorimeter, which depends on the position and arrival direction of the incoming particle and on the point of first interaction. The energy resolution for electrons and positrons is better than 2% above few hundreds GeV.

As for protons, the small number of interaction lengths of the calorimeter limits the energy resolution to about 25% or more, depending on the amount of traversed material. In **Figure *12***, the shower length distribution is shown for 1 TeV protons, selected in order to have a reliable energy measurement. An effective geometric factor can be defined as the overall geometrical factor multiplied by the selection efficiency. For a 1 TeV proton the effective geometric factor of the calorimeter can reach 5 m^2 sr.

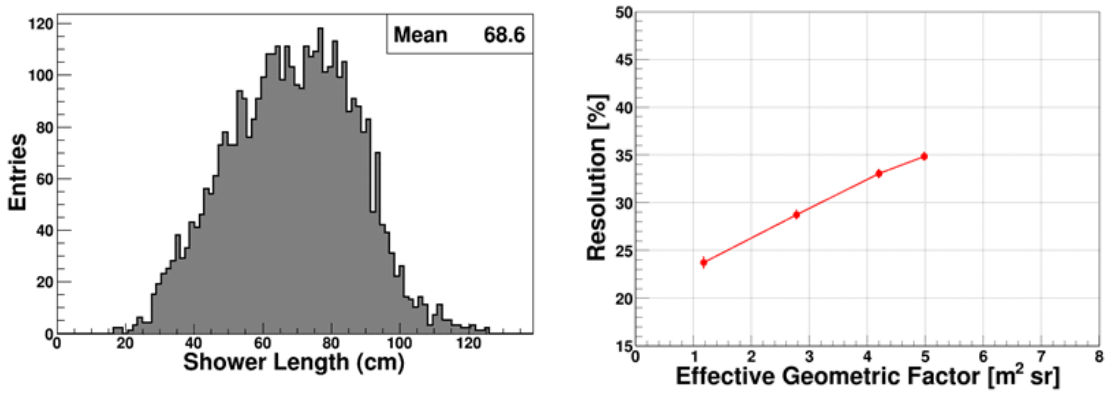

Figure 12. Left: The shower length distribution in the calorimeter for protons at 1 TeV. Right: The energy resolution as a function of the effective geometric factor for the same particles.

The energy resolution for 1 TeV protons as a function of the effective geometrical factor is also shown in Figure *12*. The resolution ranges between 24% at 1 m^2 sr to 35% at 5 m^2 sr. The simulation at higher energies shows that the energy resolution varies only slightly up to the PeV region.

In order to measure the antiparticle component of the cosmic rays the calorimeter has to discriminate between positron-initiated and proton-initiated showers. Given that the proton flux in the TeV energy range is several orders of magnitude (10^3 -10^4) higher than the positron flux, a proton rejection factor of at least 10^{-5} is needed. Shower initiated by protons develop more deeply in the calorimeter and their lateral spread is larger. Moreover, positrons are expected to lose all their energy in calorimeter, while protons lose only a fraction of it. So, the match between the energy loss in calorimeter and the rigidity measured by the tracker is an additional tool to distinguish positrons from protons.

The study of proton rejection capability requires Monte Carlo simulations with very high statistics (~10^7 events) and was not performed in preparation of this proposal. However, in the framework of the CaloCube project some preliminary simulations of the rejection capabilities for a similar calorimeter composed of 20x20x20 cubic CSI crystals

(3,6 x3,6 x3,6 cm^3) for a total depth of 39 radiation length (X_0) have been performed, showing proton rejection factors close to 10^{-5}, without tracker information. Since the ALADINO calorimeter will be much deeper, while the segmentation will be similar, we expect to reach a rejection capability close to 10^{-6}.

4.2 Spectrometer: description and performances

The ALADINO spectrometer has been designed in order to meet the target performances of an average MDR greater than 20 TV and a large acceptance. It consists of:

- A superconducting magnetic system surrounding the calorimeter. The chosen configuration is a toroid with ten circular coils. With such a configuration, characterized by a theoretical null magnetic moment, the produced magnetic field efficiently manage to bend the particle trajectories coming from the outer space.
- A tracking system composed of six layers of micro-strip silicon detector to provide a measurement of the particle trajectory into the magnet field. Each of the six detector layers are divided in ladders and arranged cylindrically around the calorimeter.

  The overall arrangement of the coils and the tracking system are shown in Figure 9.

4.2.1 MAGNET

The high resolution of the ALADINO tracker demands for high magnetic field over a large volume, therefore for the use of a superconducting magnet. With respect to permanent magnets, superconducting magnets are lighter and allow obtaining higher bending powers and geometrical acceptances. Moreover, the magnetic field is adjustable, allowing detector calibration at zero field, as well as searching for particles in a wide energy range.

Superconductors are largely used to generate high magnetic fields on Earth, but there is little experience about superconducting magnets in orbit. A superconducting magnet for an antimatter detector (ASTROMAG) was designed in the ’80 but eventually it was not launched. The Hitomi X-ray telescope, launched in February 2016 is equipped with a NbTi superconducting magnet but it is a very small device, not matching the size needed for space spectrometers. A large magnet for the AMS2 spectrometer was designed, built and successfully tested but it was decided to replace it with a permanent magnet before the launch, because of limitations in mission endurance linked to the size of the superfluid helium reservoir. At present, thanks to the developments of high temperature superconductors (YBCO, ReBCO, BSCCO or MgB_2), the limits imposed by helium cryogenics can be overcome. Recently, a European team designed a magnet system to protect astronauts from space radiations, SR2S. Despite the TRL of the radiation shield is still low, the project paved the way to the space application of high temperature superconducting magnets: the design, based on large MgB_2 toroids operating at 10 K [54], was developed applying robust and light materials for the mechanical structure; a novel, low density superconducting cable was developed, based on magnesium diboride (MgB_2)

in titanium matrix [55]; special thermal solutions were found, involving the use of sunshields, cryocoolers and cryogenic pulsed heat pipes [56]; the protection of the magnet against quenches was also studied.

The design of ALADINO magnet starts from the SR2S results: it will have a toroidal configuration in order to confine the field within the magnet, it will be wound with MgB_2 conductor (or other high temperature superconductors) and will be cooled by means of cryocoolers. Even if, in principle, the dipole moment of a perfect symmetric toroidal magnet is zero, in a real magnet a residual dipole moment is always present. This results in interaction with the geomagnetic magnetic field and consequently in torques which can modify the spacecraft attitude. Such an effect will be carefully evaluated and adequate countermeasure will be taken.

The main requirements of a superconducting magnet for space applications are lightness and reliability. The use of titanium clad MgB_2 conductors contributes to fulfill the first requirement, as its average density is 4000 kg/m^3 (it is the lightest among superconducting cables). Reliability is mainly related to stability against disturbances and quench protection. Stability is the capability of a magnet to sustain a sudden energy release without quenching. It is a delicate aspect in designing superconducting magnets operating at liquid helium temperature. However, the problem became less significant when increasing the operation temperature (due to the cubic increasing of the specific heat capacity.) A magnet, operating at 10 K, is 15 times more stable than the AMS magnet which was designed to operate at 1.8 K. Such a high stability dramatically reduces the quench probability making magnets wound with MgB_2 (as well as YBCO, ReBCO, BSCCO) reliable and consequently suitable for space application. On the contrary, if a quench occurs, its propagation velocity is reduced by the high values of the specific heat capacity. Consequently, the higher the temperature is, the more difficult the magnet protection is and an active quench protection system is mandatory. The problem of the protection of large MgB_2 space magnets was studied in the framework of the SR2S project and a solution was proposed [57].

Figure 13 shows the concept of the magnet and the field map. The ALADINO magnet has 10 coils. This number was chosen as the better compromise between low stray field and high acceptance. The shape of the coils (round, racetrack, D-shaped) will be optimized during the first phase of the project in order to

maximize the detector performances (MDR and acceptance). As a first guess it was decided to use circular coils. The coil inner diameter is 1.45 m and the cross section is 85 mm X 85 mm. The minimum diameter of the inner bore of the toroid, hosting the calorimeter, is 1 m, therefore, the overall magnet radial dimension is about 2.1 m.

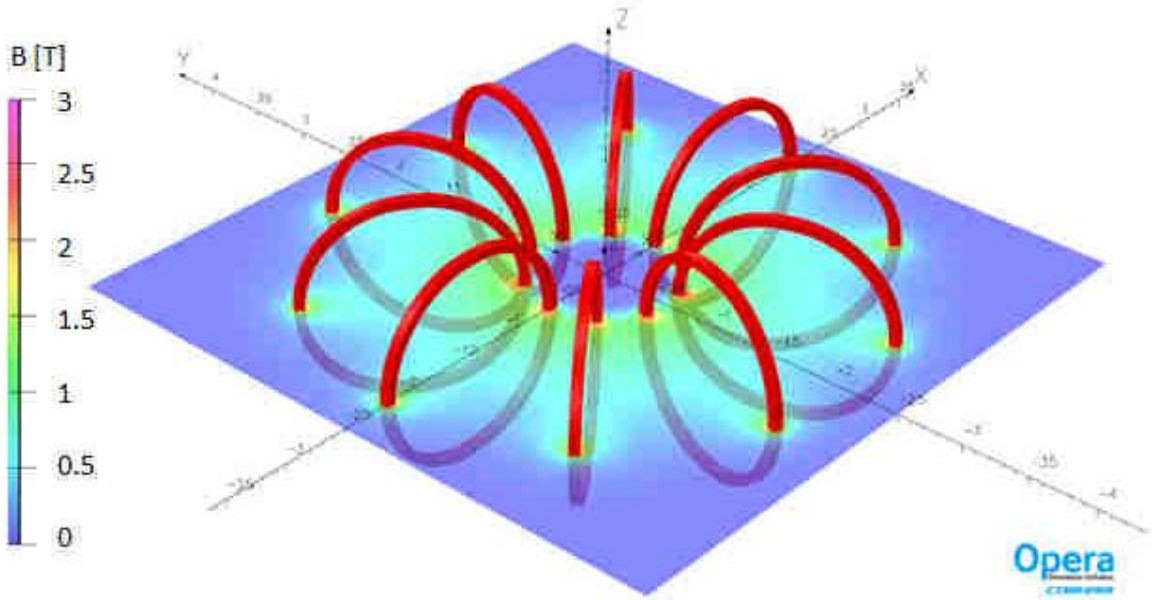

Figure 11. *Scheme of the magnet and field map*

With 437000 ampere-turns per coil, the average field on the tracker is 0.8 T and the stored energy is 3.9 MJ. The maximum field at the conductor is limited to 3 T. At 3 T and 10 K, the prototype Ti-MgB_2 conductor developed for SR2S is able to carry about 270 A/mm^2. Using a reasonable safety margin, the current density in the superconducting tape is limited to 180 A/mm^2. By using the tape developed for SR2S (1.5 mm^2), the operating current could be 270 A and the magnet inductance about 100 H. In parallel to the Ti-MgB_2 tape, a pure aluminium strip has the function to protect coils in case of quench. In the described configuration, the mass of the conductor, including aluminium and electrical insulation is about 940 kg. The mass of the magnet, including the mechanical structure is 1500 kg. The main characteristics of the magnet are shown in Table *2*.

Table 2. *Main characteristics of the magnet.*

Number of coils	10
Total current per coil	437000 amp-turns
Operating current	270 A
Inductance	100 H
Average magnetic flux density	0.8 T
Cold mass	1500 kg

4.2.2 MAGNET OPERATION AND CRYOGENICS

The most appropriate mode to operate a superconducting magnet in space for long periods is the persistent mode: the magnet is charged using a power supply up to the

nominal current, then the superconducting circuit is closed using a superconducting switch. The power supply is ramped down but the current continues flowing in the magnet. At the end, in order to minimize the heat load at low temperature, the current leads are disconnected from the magnet. The described procedure is commonly used in MRI magnet and a system for space operation was developed and successfully tested for the AMS magnet.

Persistent mode requires high inductance and low resistance. Resistance could come from joints and conductor flux creep and/or defects. Technology to make superconducting joints between MgB_2 cables does exist, therefore only conductor residual resistance has to be taken into account. In order to keep the magnetic field within 99% it could be necessary to fill up on current every 4 month. Fill up operation can be done either by direct connection as described above for the magnet charging or via magnetic flux pump.

The conceptual cryogenic design, whose schematics is reported in Figure *14*, is based on the interception of the thermal radiation power coming from several sources by a series of thermally connected radiation shields and links and a renewable cooling source provided by a cryocooler. This conceptual design concerns the steady-state regime of the magnet upon which the quench protection and cooldown scenario will be based.

This superconducting system receives heat flux from three main sources: the space (sun and eventually planets), the calorimeter and an ensemble of detectors (ToF and trackers) that have to be intercepted to maintain the coils in their superconducting state. Concerning the thermal interception of the radiation heat flux coming from “space”, a typical passive thermal shield method, i.e. a thermal sunshield, is retained. This sunshield will be located far from the magnet, as an umbrella-type, to intercept a large amount of the heat flux. In space applications, sunshields made of V-groove layers are generally used. These V-grove shields are made of different reflective layers oriented with different angles to each other allowing a better extraction of the heat at each layer. Moreover in space the temperature of the universe helps cooling the different layers that compose the sunshield. This solution has been used for the Plank satellite and the James Webb telescope. Each layer is made of Kapton® covered with aluminum (emissivity=0.1). The first layer (the one facing directly the sun or the main source of heat) is covered with an Optical Solar Reflector (OSR) to reflect most of the incoming heat flux.

An overall computation has been performed to estimate the heat fluxes absorbed by such a sunshield made of 2 V-groove layers with the first one covered with OSR (absorption = 0.07 and emission = 0.86).

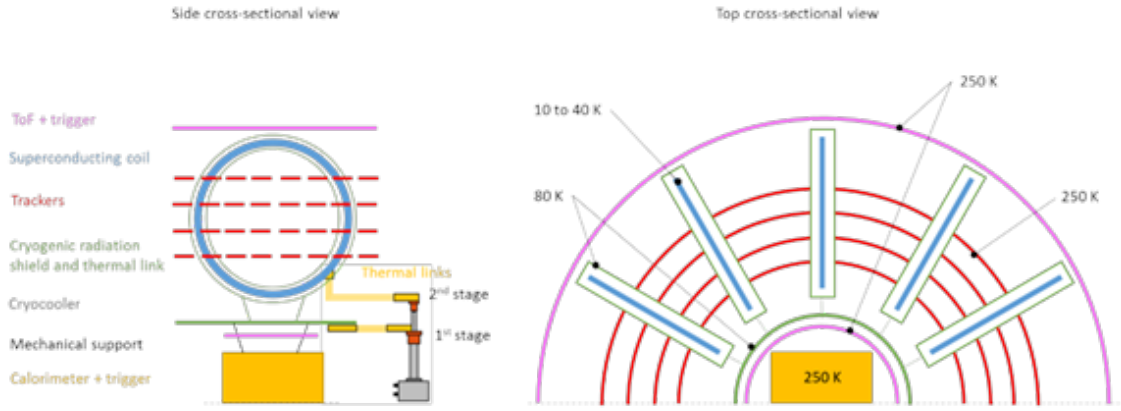

Figure 12. *Schematics of the conceptual cryogenic design.*

Temperature of about 60 K has been calculated on the surface of the cold side layer and a heat flux density of 80 mW/m². This heat flux will be intercepted by the external ToF surface and will enter in the power budget to maintain the ToF at its working temperature of 250 K. As the two cross-sectional views from figure 2 show, the superconducting coils are subjected to multi-directional thermal radiation from the calorimeter, the ToF and the tracker that are supposed to be functioning at a temperature of 250 K. To maintain these coils at a temperature between 10 K and 40 K (the range of working temperature envisaged for the superconductors), a set of two thermal shield systems will be placed between the 250 K radiation surfaces and the coils. Due to the multi-directional thermal radiation, the two shields will surround each superconducting coil to maximize the absorption rate. The first one, directly facing the 250 K surfaces, will be actively maintained at 80 K by a cryocooler and the second one, thermally passive, will be at a temperature close to the magnet working temperature (see Fig.14). The principle of the cryogenic design is to have a central thermal link surrounding the calorimeter cooled by the cryocooler distributing the cooling power to each 80 K thermal shield. These 80 K shields will be thermally connected to the central thermal link by pulsating heat pipes, much lighter and efficient than pure copper straps, to minimize the weight. The 80 K thermal shield will be composed of a light structure supporting a cryogenic multi-layers insulation (MLI) with 10 to 20 layers. Generally, the performance of such MLI is 1 W/m² with a clean room assembly. For the ALADINO configuration, the maximum radiation power to be extracted to maintain the shield at 80 K is in the order of 50 W. This heat load will be absorbed by the first stage of the cryocooler (see Fig. 14). To reduce the heat fluxes coming from the 80 K thermal shield, the second shield will be also composed of 10 to 20 layers of MLI and will be directly wrapped around the coils. From 80 K, the MLI performance is about 0.1 W/m² which represents a heat load of 2 W on the entire coils system at a temperature of 40 K to 10 K. Mechanical supports will be necessary to maintain the entire assembly together. These structural pieces will conduct heat from the 250 K regions to the cryogenic ones. To reduce the amount of thermal conduction, low

heat conductivity and high mechanical characteristics materials, like G-10 glass-fiber/epoxy composite, are envisaged. These materials have a maximum compression stress of roughly 40 MPa and to sustain the high acceleration of the launch (roughly 10 g), the number and cross-sectional area will have to be designed carefully. Nevertheless, a first estimate of the heat load can be made taking the assumption that a maximum acceleration of 1 g will be sustained by these supports. It represents 10 W of heat on the 80 K thermal shields and 1 W on the coils. The current overall weight of a powerful cryocooler with its compression system is around 100 kg and one can estimate that the mechanical supports would be an order of magnitude lighter.

4.2.3 TRACKER

Tracking with a O(μm) precision is achieved in ALADINO using double side silicon microstrip detectors.

Originally developed in the ‘80s for micro-vertex detectors in the High Energy Physics experiments at colliders, the precursor flight of the AMS experiment on the shuttle Discovery in 1998 has first demonstrated that thin, O(300μm), silicon microstrip detectors can be successfully operated for tracking in space. Precision measurement of particle coordinates is accompanied in silicon microstrip detectors by light weight, minimum material along the particle trajectory (thus reduced possibility of particles scattering in the detector material), absence of consumables (opposite to gas detector), and relatively low operating voltages (≈70 V). Silicon trackers have been therefore adopted in calorimetric experiments (Agile, Fermi, DAMPE) or magnetic spectrometers (PAMELA, AMS-02), and ≈90 m^2 of silicon detectors are currently operating successfully in space in long term missions.

The ionization loss of singly charged particles traversing the fully depleted, reverse-biased 300 μm thick sensor is described by a Landau distribution with a peak energy loss of 22,000 electron-hole pairs. The opposite sign +/- charge carriers drift rapidly (10-25 ns) in the electric field to the two surfaces (p/n) where the accumulated charge on the metalized strips (p+/n+) is fed to the front-end electronics. The position of the particle is determined by the relative signal levels observed at the readout strip positions, whereas the charge magnitude can be assessed from the amplitude of the total energy deposit, which is proportional to Z^2.

The design of the ALADINO tracking system benefits from the experience of AMS and PAMELA experiments. In its baseline design it is composed of 7540 high resistivity sensors, 95x95 mm^2 each, for a total detector surface of about 68 m^2. The sensor design uses capacitive charge coupling with floating strips in order to get optimal spatial resolution with a reduced number of readout channels. We plan to use a strip pitch of 25 μm and a readout pitch of 100 μm, reading out only one every 4 strips.

The silicon sensors are grouped together for readout and biasing into *ladders*, made of a variable number of sensors (from 2 to 7) to match the size of the different tracker planes. To reduce the material in the tracking volume, front-end electronics is located at the ladders end. For the p-strips, the daisy chain is then provided through direct bonding

from sensor to sensor, while for the transversal n-strips a metalized Upilex film running over the ladder length is used to connect to the corresponding front-end electronics. Each ladder will have 14 readout chips (64 channels each) for a total of 896 readout channels on each side, with an estimated power consumption of 0.5 W. Figure *15* shows the two sides of a ladder, as build for the AMS-02 detector with small (40x70 mm^2) silicon detector. In ALADINO a total of 1400 ladders, with length up to seven silicon detectors for a total of 66.5 cm, will be disposed on six planes surrounding the calorimeter as visible in Figure *9*. The ladders will be mounted on support planes made of a low density aluminum honeycomb structure enclosed within thin Carbon Fiber Reinforced Polymer (CFRP) skins.

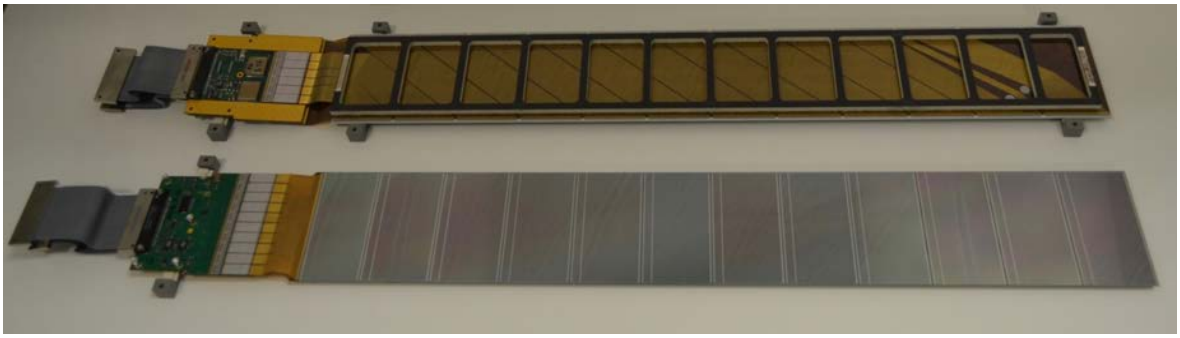

Figure 15*. n (top) and p (bottom) sides of a 12 sensors AMS-02 ladder.*

The readout pitch, together with low noise front-end electronics will ensure a position resolution of about 3 μm for normal particle incidence: a similar result has already been obtained with the PAMELA short ladders (Fig. 16 left), while AMS-02 has demonstrated the possibility to use long detector modules (up to 60 cm, in ALADINO we use up to 66.5 cm) with a resolution better than 10 μm. With a moderate R&D activity to optimize the readout electronics, we plan to obtain the design value of 3 μm on long detector module, with a limited power consumption of about 0.3 mW per channel.

Furthermore the dynamic range of the front-end will extend, similar to the AMS-02 [77] such as to reach at least the Oxygen signal amplitude without saturation. In order to fully exploit the intrinsic resolution of the detectors, and given the worsening of the resolution with the track incident angle, a peculiar ladder orientation has been devised, as shown in the middle panel of Figure 16.

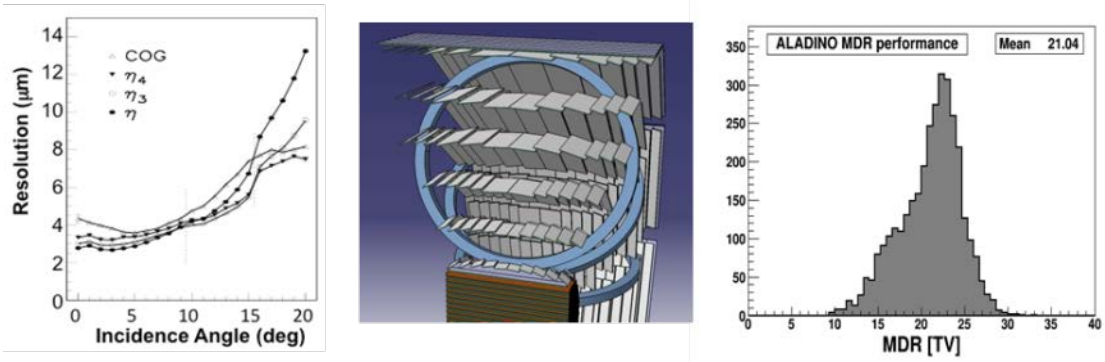

Figure 13. *Left: Spatial resolution as a function of the incident angle in the PAMELA experiment. Middle: silicon ladder orientation in ALADINO experiment. Right: MDR distribution of the spectrometer.*

4.3 Spectrometer Performance

A first, very approximated, analysis of the spectrometer performance can be obtained by means of a simple analytical formula [58]:

$$\delta k = \frac{\Delta x}{L^2}\sqrt{\frac{720}{N+4}}$$

This approach holds for space position measurements with constant resolution along a trajectory in a uniform magnetic field. *k* is the curvature (i.e. the inverse of the curvature radius), Δx is the position measurement error, *L* the projected length of the track onto the bending plane and *N* the number of points along track. The spatial resolution in ALADINO is Δx=3 μm for vertical incident particles; the number of points is *N* = 6; the minimum level arm *L* can be taken as ~1.7 m; the magnetic field is not uniform but in a first approximation we can take the average value of 0.8 T. With this values a MDR ~ 27 TV is obtained.

The real performance evaluation should take into account the field unevenness, the position tracking resolution as a function of the incident angle, and the features of the isotropic cosmic rays fluxes incident on the experiment. The detailed study has been obtained through a particle tracking Monte Carlo simulation including the magnetic field configuration and the tracking system geometry. Due to the not uniform field and the complex arrangement of the silicon detectors the rigidity resolution depends on the position and arrival direction of the particles. A flux of isotropic particles incident on the external surface of the ALADINO spectrometer has been simulated in order to obtain the MDR distribution. The result is reported in Figure 16. The MDR values obtained range between 10 and 35 TV with a mean value greater than 20 TV. From the AMS and PAMELA experience we know that charge sign separation to identify antiparticles respect to the particle counterpart can reliable arrive to ~MDR/4 in rigidity. That means ALADINO experiment can measure antiproton and positron fluxes up to 5 TeV.

4.4 ToF

The ALADINO ToF System is made of four layers of 0.8 cm thick plastic scintillators, placed in pairs before and after the tracker. The outer layers are mounted on ten 190 x 130 cm^2 planar supports, each containing thirteen counters 10 cm wide by 190 cm long aligned with the detector axis and 19 counters 10 x 130 cm^2 perpendicular to the detector axis. The inner layers are mounted on ten 90 x 30 cm^2 planar supports, each containing three counters 10 cm wide by 90 cm long counters aligned with the detector axis and nine counters 10 cm wide by 30 cm long perpendicular to the detector axis. The mounting of the counters is such as to avoid dead space for trigger purposes. Counters are read out on each end by Silicon Photomultipliers (SiPMs) (HAMAMATSU S13360-3050VE or equivalent surface mounted type, insensitive to magnetic fields). The counters are contained in a carbon fiber cover for light tightness.

From the measurement of the 135 cm long AMS-01 scintillator counters [TOF-AMS01], the attenuation of light along the counter can be described by the function:

$$N_{pe}(x) = N_{pe-max}\left[D \cdot e^{-x/\lambda} + (1-D) \cdot e^{-(2L-x)/\lambda}\right]$$

where x is the distance from one end, $N_{pe}(x)$ is the number of photoelectrons produced at distance x form the end, $N_{pe\text{-}max}$=530 is a normalization parameter, such that N_{pe}=350 at the center of the counter, D=0.85 is the fraction of direct light seen on one end of the counter and λ=200 cm is the attenuation length in the scintillator. The corresponding time resolution at one side of the counter is:

$$\sigma(x) = \sqrt{\frac{\sigma_1^2}{N} + \frac{\sigma_2^2 x^2}{N} + \sigma_3^2}$$

where σ_1=2000 ps is the resolution due to the PM signal shape and to the trigger electronics, σ_2=20 ps/cm is the resolution due to the dispersion of the photon path lengths, x is the distance from the side, σ_3=90 ps is the electronic noise and N is the number of photoelectrons produced in the PMTs of the side.

The mean time resolution of one counter is:

$$\sigma_t(x) = \frac{\sqrt{\sigma_{t1}^2 + \sigma_{t2}^2}}{2}$$

where σ_{t1} and σ_{t2} are the time resolution of the two ends of the counter.

The expected time resolution as a function of the position along the counter is shown in Figure *17* (left) for 190 cm long and 30 cm long counters. A fast simulation of the performances of the ALADINO ToF system shows that the identification of anti-deuterons against anti-protons is possible in the kinetic energy region below 0.8 GeV/n (R<2.9 GV), as shown in Figure *17* (right).

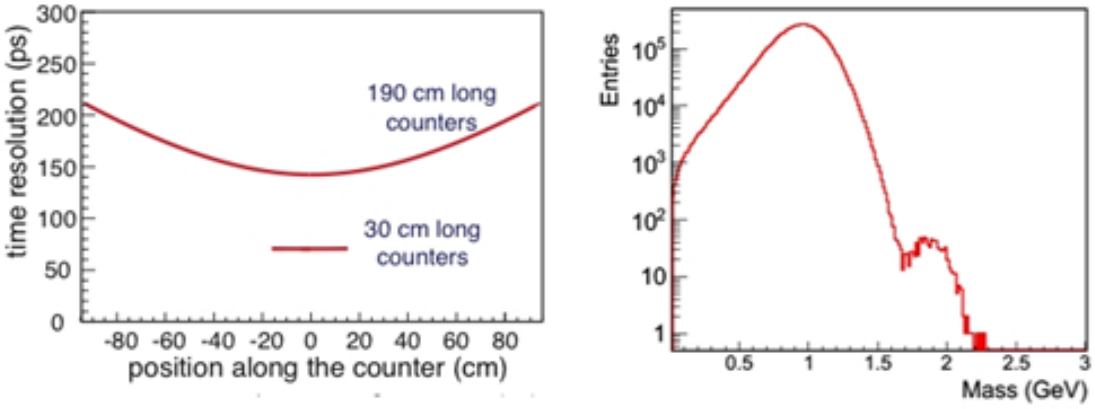

Figure 14. *Left:* *Mean time resolution as a function of the particle hit position along the counter for 200 cm (red) and 35 cm (black) long counters.* ***Right:*** *Reconstructed mass for antiparticles with 2.4<R<2.7 GV (0.6<E_{kin}<0.7 GeV/n), with 10^8 simulated antiprotons and 10^3 simulated antideuterons. The anti-deuterons reconstructed mass peaks at 1.88 GeV and is quite well separated from the antiproton background*

5 MISSION REQUIREMENTS

5.1 Orbital Requirements

Access to space is necessary to avoid antimatter background from CR collisions with the Earth's atmosphere. Geomagnetic flux modulation, back-scattered albedo particles, and geomagnetically trapped particles represent known limiting factors for low-Earth orbiting experiments that affect acquisition capabilities (via radiation damage) and CR flux (via Galactic CR flux suppression at p/|Z|<~30 GV). The latter is critical for the observational goals related to low energy anti-deuteron, anti-helium measurements and Heliospheric studies. All these issues can be resolved by a high-Earth orbit or L2 orbit. Moreover, these type of orbits are most appropriate for a proper thermal environment required by the scientific payload. It is important to note that no active attitude control is required for the mission, provided that appropriate sky coverage is guaranteed.

5.2 Weight and Power Budget

About 2 Tons of the mass budget are allocated to the magnetic system, including the cryogenic and insulation. The next heavy part is the LYSO crystal of the calorimeter, for a weight of 2.3 Tons including 300 kg of mechanical structure. The Tracker and ToF systems are estimated to about 1.5 Ton, and about 500 kg are allocated for the power, readout and control electronics of all the subsystems. The current total mass estimate is thus about 6.4 Tons for the experimental apparatus.

The ALADINO detector, although with an high acceptance (of the order of 3 m^2 sr) has a limited number of readout channels, thanks to the innovative design, but still is quite

demanding in term of power for a space application. The most consuming detector subsystem is the Tracker, with 251.000 channels and a total power consumption of about 1 kW. The Calorimeter is read-out through 31.000 electronics channels, with an estimated power consumption of about 200 W. The ToF, with about 2000 channels of high speed electronics has a power consumption of about 400 W. The cryogenic system will consume about 1 kW to keep the magnets coil at the nominal operating temperature. The total power budget is thus estimated to 2.8 kW.

5.3 Operational Requirements

The experiment must be operational 24 hours a day, 7 days a week, and 365 days a year without human interventions or on-orbit maintenance activities. It must provide a continuous stream of data at a rate of the order of ~20 Gigabits per second. This requires the development of sophisticated onboard data reduction and compression techniques and appropriate hardware. Requirements for offline activities, from slow-control monitoring to high-level physics, are coordination and man power. The coordination among international teams of scientists is an essential requirement for the definition, implementation, and accomplishment of the mission. It is expected that the science management will follow the model of high-energy physics collaborations. Such a model has been successfully validated in several recent astro-particle physics missions in space.

6 TECHNOLOGY DEVELOPMENT REQUIREMENTS

One of the key item for the success of an instrument such as ALADINO is the optimal design of the space platform and its integration with the payload system: a coordinate and joint effort is needed since the early stage of the design process, in order to design the two systems with an optimal integration, with the goal of the best use of the limited mass and power budget in order to maximize the detector performance and achieve the physics goal of the mission. This will require a detailed study of the possible launch vehicle that are and will be available in the time frame of the project, estimated in not less than fifteen years after an eventual proposal approval.

As today the most relevant technological challenge of the ALADINO project is the use of a high temperature superconducting magnet, and in particular the design and operation of the superconducting magnet, and its cryogenics system for space application. Given the complexity of such a project, we have evaluated a period of 18 months for the Preliminary Design Report, 5 years of R&D activity and 6 years for the construction, test and integration of the flight magnet.

The detectors technology (silicon Tracker, scintillator based Time of Flight and crystal Calorimeter) has been already successfully used in space, and pose no major problem in the current design. However given the tight constraints - power and mass budget, mechanical compactness - the detector will be operated at a relatively low temperature (250 K). This will require a moderate R&D effort, estimated in a three years

period, to properly assess the detector performance and the optimization of the design and assembly technique. Completed the design and prototype phase, the assembly and test of the detector, including the space qualification tests, will cover a 5 years period.

The magnet and detector integration will require one year of activities, with a second year devoted to ground performance tests and calibration on particle's beam. The space qualification of the whole system will require a third year, to bring the whole system to be ready for launch.

7 OTHER INFORMATION

The ALADINO proponents have developed, in more then thirty years of experience in construction, deployment and operation of space-borne CR spectrometers, deep relationships with European space Agencies (ASI in Italy, CNES in France, DLR in Germany, etc.), and with NASA, NSPO, ROSKOSMOS, JAXA and CNSA. Moreover, continuous support has been provided by European and International Institutes promoting particle physics in several Countries. The space detector in which some or all of the proponents have been involved include AMS-01 (1994-1998), PAMELA (1998-now), AMS-02 (1999-now), FERMI (2000-now), DAMPE (2013-now). The ALADINO proponents intend to pursue a strong involvement of these Agencies and founding Institutions in the Project.

8 REFERENCES

[1] S.I. Blinnikov, A. D. Dolgov, K. A. Postnov, 2015, Phys. Rev. D 92, 023516
[2] P. Salati, 2015, P., Proc. 17th Lomonosov Conference, Moscow [arXiv:1605.01218]
[3] P. Blasi, 2014, Braz. J. Phys. 44, 426; [arXiv:1312.1590, see also arXiv:1412.8430]
[4] I.A. Grenier, J. H. Black, A. W. Strong, 2015, Ann. Rev. A&A 53, 199
[5] M. Potgieter, 2013, Living Rev. Solar Phys., 10, 3
[6] K. Abe et al., 2012 (BESS Collaboration), Phys. Rev. Lett. 108, 051102
[7] A.G. Cohen, A. D. Rujula, S. L. Glashow, 1998, Astrophys. J. 495, 539
[8] A.D. Sakharov, 1967, JTEP Lett. 5, 24
[9] C. Bambi & A. D. Dolgov, 2007, Nucl. Phys. B 784, 132
[10] B. Ostdiek, 2015, Phys. Rev. D 92, 055008
[11] J. Hisano, K. Ishiwata, N. Nagata, 2015, JHEP 1506, 097
[12] M. Cirelli et al., 2014, JHEP 1410, 033
[13] N. Masi & M. Ballardini, 2015, [arXiv:1509.00058]
[14] P. Serpico, 2011, Astropart.Phys., 39-40, 2–11
[15] P. Serpico, 2015, Proc. 34th Int. Cosmic Ray Conf., PoS(ICRC2015)009, [arXiv:1509.04233]
[16] G.V. Kulikov & G.B. Khristiansen, 1958, J. Exp. Theor. Phys. 35, 635
[17] J.R. Hoerandel, 2004, Astrop. Phys. 21, 241 and references therein
[18] D. D'Enterria et al., 2011, Astrop. Phys. 35 98

[19] E.S. Seo, 2012, Astrop. Phys. 39-40, 76
[20] O. Adriani et al, 2014 (PAMELA Collaboration), Phys. Rep. 544, 323-370
[21] O. Adriani et al., 2009a, (PAMELA Collaboration), Nature, 458, 607
[22] M. Ackermann et al., 2012, Phys. Rev. Lett. 108, 011103
[23] M. Aguilar et al. (AMS-02 Collaboration), 2013, Phys. Rev. Lett. 110, 141102
[24] P.S. Marocchesi et al., 2016, J. Phys. Conf. Ser. 718, 052023
[25] J. Chang et al., 2014, Chinese J. of Space Sci. 34, 550
[26] E.S. Seo et al., 2014, Adv. Space Res. 53, 1451
[27] M. Ibe et al., 2013, JHEP 1307, 063
[28] I.Cholis & D. Hooper, 2013, Phys. Rev. D 88, 023013
[29] P. S. Bhupal Dev et al., 2014, Phys. Rev. D 89, 095001
[30] T. Linden & S. Profumo, 2013, ApJ 772, 18
[31] L. Accardo et al., (AMS-02 Collaboration), 2014, Phys. Rev. Lett. 113, 121101
[32] J. Berdugo et al., 2015, arXiv:1510.01221
[33] M. Cirelli et al., 2015a, JCAP 1510, 026
[34] B.Q. Lu, H. S. Zong, 2016, Phys. Rev. D 93, 103517
[35] M. Aguilar et al. (AMS-02 Collaboration), 2016, Phys. Rev. Lett 117, 091103
[36] T. Aramaki et al., 2016, Phys. Report. 618, 7, 1-37
[37] M. Cirelli et al., 2014b, JHEP 1408, 009
[38] E. Carlson et al., 2014, Phys. Rev. D 89, 076005
[39] H. Fuke, et al, (BESS Collaboration), 2005, Phys. Rev. Lett. 95
[40] M. Aguilar et al. (AMS-01 Collaboration), 2002, Physics Reports 366, 331
[41] T. Kobayashi et al., 2004, The Astrophys. Jour. 601 (2004) 340
[42] F. Aharonian et al., 2009, Astron. & Astrophys. 508, 561
[43] D. Staszak, 2015, Proceedings of 34th Int. Cosmic Ray Conf., Pos(ICRC2015) 411
[44] H.S. Ahn et al., 2010, Astrophys. J. Lett. 714, L89
[45] M. Aguilar et al. (AMS-02 Collaboration), 2015a, Phys. Rev. Lett 114, 171103 and references therein
[46] J.R. Hoerandel, 2003, Astrop. Phys. 19, 193
[47] T.Gaisser, T. Stanev and S. Tilav, 2013, Front. Phys. 8, 748
[48] N. Mori et al., 2013, Nucl. Instrum. Meth. A 2013, 732, 311-315
[49] D. Alvisi et al., 1999, Nucl. Instrum. Meth. A 437, 212-221
[50] J. Alcaraz et al., 2008, Nucl. Instrum. Meth. A 593, 376-398
[51] S. Straulino et al., 2006, Nucl. Instrum. Meth. A556, 100-114
[52] S. Agostinelli et al., 2003, Nucl. Instrum. Meth. A 506 (2003) 250
[53] J. Allison et al., 2006, IEEE Trans. Nucl. Sci. 53, 270
[54] R. Musenich et al, 2014, IEEE Transaction on Applied Superconductivity, 24 (3)
[55] R. Musenich et al. 2016, IEEE Transaction on Applied Superconductivity, 26 (4)
[56] R. Bruce & B. Baudouy, 2015, Physics Procedia, 67, 2015.
[57] F.P. Juster & C. Berriaud, 2015, SR2S report SR2S-WP31-D31.4
[58] K.A. Olive et al. (Particle Data Group), 2014, Chin. Phys. C, 38, 090001.
[59] G. Aad et al. (ATLAS Collaboration), 2015, Phys. Rev. D 91, 052007
[60] A.Abdo et al., 2009, Phys. Rev. Lett. 102, 181101
[61] M. Aguilar et al. (AMS-02 Collaboration), 2014, Phys. Rev. Lett. 113, 221102
[62] M. Aguilar et al. (AMS-02 Collaboration), 2015b, Phys. Rev. Lett 115, 211101 and references therein
[63] J. Alcaraz et al. (AMS-01 Collaboration), 1999, Phys. Lett. B 461, 387 and references therein

[64] T. Aramaki et al., 2014, Astropart. Phys. 59, 12
[65] M. Cirelli, et al, 2009, Nucl. Phys.B 813, 1
[66] M. Cirelli, et al, 2013 Nucl. Phys. B 873, 530
[67] M. Cirelli, 2015b, Proc. 34th ICRC, PoS(ICRC2015)014 [arXiv:1511.02031]
[68] A.Ibarra, A. S. Lamperstorfer and J. Silk, Phys. Rev. D 89, no. 6, 063539 (2014)
[69] M. Ibe et al.,2013, JHEP 07(2013)063
[70] Z.P. Liu, Y. L. Wu and Y. F. Zhou, 2013, Phys. Rev. D 88, 096008
[71] S.J. Lin, Q. Yuan and X. J. Bi, 2015, Phys. Rev. D 91, no. 6, 063508
[72] C. Lopez, D. Savage, D. Spolyar and D. Q. Adams, 2016, JCAP 03, 033
[73] Smoot et al., Phys.Rev.Lett. 35 (1975) 258-261
[74] Cristinziani, Nucl.Phys.Proc.Suppl. 113 (2002) 195-201
[75] Salati 2016: arXiv:1605.01218
[76] Aramaki et al., Phys.Rept. 618 (2016) 1-37
[77] Saouter 2013: PoS Vertex2014 (2015) 028